



HAL
open science

Proteomic analysis identified LBP and CD14 as key proteins in blood/biphasic calcium phosphate microparticle interactions

Lun Jing, Solène Rota, Florian Olivier, David Momier, Jean-Marie Guignonis, Sébastien Schaub, Michel Samson, Jean-Michel Bouler, Jean-Claude Scimeca, Nathalie Rochet, et al.

► To cite this version:

Lun Jing, Solène Rota, Florian Olivier, David Momier, Jean-Marie Guignonis, et al.. Proteomic analysis identified LBP and CD14 as key proteins in blood/biphasic calcium phosphate microparticle interactions. *Acta Biomaterialia*, 2021, 127, pp.298-312. 10.1016/j.actbio.2021.03.070 . hal-03357728

HAL Id: hal-03357728

<https://hal.science/hal-03357728>

Submitted on 24 May 2023

HAL is a multi-disciplinary open access archive for the deposit and dissemination of scientific research documents, whether they are published or not. The documents may come from teaching and research institutions in France or abroad, or from public or private research centers.

L'archive ouverte pluridisciplinaire **HAL**, est destinée au dépôt et à la diffusion de documents scientifiques de niveau recherche, publiés ou non, émanant des établissements d'enseignement et de recherche français ou étrangers, des laboratoires publics ou privés.



Distributed under a Creative Commons Attribution - NonCommercial 4.0 International License

PROTEOMIC ANALYSIS IDENTIFIED LBP AND CD14 AS KEY PROTEINS IN BLOOD/BIPHASIC CALCIUM PHOSPHATE MICROPARTICLE INTERACTIONS

Lun Jing ^{a, b}, Solène Rota ^c, Florian Olivier ^d, David Momier ^c, Jean-Marie Guignonis ^{a, b},
Sébastien Schaub ^{c, e}, Michel Samson ^{a, b}, Jean-Michel Bouler ^f, Jean-Claude Scimeca ^c,
Nathalie Rochet ^c, Patricia Lagadec ^{c*}

Running title: LBP and CD14 are key proteins in blood/BCP interactions

^a Université Côte d'Azur, UMR E-4320, CEA/DRF/BIAM, Faculté de Médecine, Nice, France

^b Université Côte d'Azur, Plateforme de protéomique "Bernard Rossi", Faculté de Médecine, Nice, France

^c Université Côte d'Azur, CNRS (UMR 7277), Inserm (U1091), iBV, Nice, France

^d Université d'Orléans, CNRS (UMR7374), ICMN, Orléans, France.

^e Université de la Sorbonne, CNRS (UMR 7009), LBDV, Villefranche-sur-mer, France.

^f Université de Nantes, CNRS (UMR 6230), CEISAM, Nantes, France

***Correspondence to Patricia Lagadec:**

E-mail : lagadec@unice.fr

Address : Institut de Biologie Valrose (iBV), UFR de Médecine Pasteur, 28 avenue de Valombrose, 06107 Nice Cedex 2, France.

Tel : +33 493 377 795

ABSTRACT

Immediately upon implantation, scaffolds for bone repair are exposed to the patient's blood. Blood proteins adhere to the biomaterial surface and the protein layer affects both blood cell functions and biomaterial bioactivity. Previously, we reported that 80-200 μm biphasic calcium phosphate (BCP) microparticles embedded in a blood clot, induce ectopic woven bone formation in mice, when 200-500 μm BCP particles induce mainly fibrous tissue. Here, in a LC-MS/MS proteomic study we compared the differentially expressed blood proteins (plasma and blood cell proteins) and the deregulated signaling pathways of these osteogenic and fibrogenic blood composites. We showed that blood/BCP-induced osteogenesis is associated with a higher expression of fibrinogen (FGN) and an upregulation of the Myd88- and NF- κ B-dependent TLR4 signaling cascade. We also highlighted the key role of the LBP/CD14 proteins in the TLR4 activation of blood cells by BCP particles. As FGN is an endogenous ligand of TLR4, able to modulate blood composite stiffness, we propose that different FGN concentrations modify the blood clot mechanical properties, which in turn modulate BCP/blood composite osteoactivity through TLR4 signaling. The present findings provide an insight at the protein level, into the mechanisms leading to an efficient bone reconstruction by blood/BCP composites.

Key words: LC-MS/MS, stiffness, monocytes, Fibrinogen, TLR4, LBP/CD14

Introduction

Bone defects beyond a certain size threshold have no intrinsic ability to heal, rendering the management of large bone defects the most challenging issue for orthopedic surgeons. Filling large bone defects with scaffolds or with biomaterial composites is often required as alternatives or additives to the “gold standard” autologous bone graft [1, 2]. Immediately upon implantation, bone scaffolds are exposed to the patient’s blood, leading to blood clotting concomitant with an acute phase inflammatory reaction [3-7]. The nature and intensity of this inflammation is crucial to fight a potentially dangerous exogenous material, restore homeostasis (or not), and promote (or not) healing. The structure of blood clot [4, 8], and the physicochemical properties of the bone substitute [3, 5, 7, 9], also deeply influence the biocompatibility and the bone healing. But, in spite of blood/biomaterial interactions having such a pivotal role, there is a surprising paucity of scientific literature that study these interactions at the molecular levels.

Among biomaterials, synthetic calcium phosphate (Ca-P) ceramics have been widely used for bone regeneration because of their osteoinductive properties [2, 9-13], and among Ca-P biomaterials, biphasic calcium phosphate (BCPs) ceramics are considered as the gold standard in bone reconstruction surgery [2, 14, 15]. Therefore, BCP which is made of a mixture of hydroxyapatite (HA) and β -tricalcium phosphate (β -TCP), are frequently used to fill bone defects where they encounter blood. We reported before, that BCP microparticles 80-200 μ m embedded in a blood clot induced ectopic woven bone formation in mice, when BCP microparticles 200-500 μ m mainly generated fibrous tissue [11]. Using a transcriptomic approach we previously showed *in vitro* and in 3D that the Toll-like receptor 4 (TLR4) was involved in the inflammatory process triggered in blood cells by 80-200 μ m BCP particle interactions, which resulted in the increase of IL-1 β and IL-6 gene expression [16]. TLRs are

single, transmembrane, non-catalytic receptors usually expressed on sentinel cells such as monocytes/macrophages (M/M). They are a panel of conserved pattern-recognition receptors (PRR) that are activated by a variety of pathogen-associated molecular patterns (PAMPs), thus initiating an innate immune response and inflammation in higher animals [17, 18]. TLR4 was originally described to recognize lipopolysaccharides (LPS) from Gram negative bacteria. LPS-activated TLR4 induces intracellular signaling in collaboration with other molecules, such as LPS-binding protein (LBP) and cluster of differentiation 14 (CD14). Once the sequential action of LBP and CD14 has promoted the formation of the activated TLR4/MD-2 (Myeloid Differentiation factor 2) heterodimer on the cell surface, the activated complex recruits the adapter molecule MyD88 (Myeloid differentiation primary response 88) which binds Interleukin-1 receptor-associated kinases 2 and 4 (IRAK2 and IRAK4) within the cytoplasm of cells, inducing the activation of the nuclear factor- κ B (NF- κ B). Currently, TLR4 has also been identified as a ‘danger-sensing’ receptor [18]. As a result, in addition to LPS, TLR4 can be also activated by many types of host-derived molecules including released intracellular proteins (e.g., S100A8/A9, high-mobility group protein B1), extracellular matrix components, and soluble mediators (e.g., fibrinogen) [18, 19]. These molecules represent members of a recently identified family of proteins, termed “alarmins”, which serve as mediators of inflammation and are expressed or released in response to tissue damage [20]. Because patients having a large bone repair do not usually exhibit infectious disease, the stimulation of the TLR4 signaling in such case may results from endogenous TLR4 ligand rather than being due to the presence of bacterial products.

After implantation, blood proteins rapidly adhere to the biomaterial surface [3, 5, 21, 22]. The pattern of adsorbed proteins differs among the surfaces, and varies over time. Subsequent interactions of the biomaterial with blood cells are likely to be modified by this protein layer,

as well as by the resulting secreted mediators. Therefore, the identification of these molecules would be of great help in bone tissue engineering. Proteomics, as a hypothesis-free approach, is a useful tool for discovering novel molecules. So, in the present study, we investigated protein expression profiles during blood/BCP interactions *in vitro* and *in 3D* using liquid chromatography coupled to mass spectrometry (LC-MS/MS). First we compared the expression profiles of plasma and blood cell proteins between blood/BCP composites versus blood clot in semi-quantitative label-free experiments and analyzed the deregulated signaling pathways. Second, we performed quantitative proteomic studies between osteogenic (BCP 80-200 /blood) and fibrogenic (BCP 200-500/ blood) composites to identify the ‘alarmins’ involved in the activation of the TLR4 signaling cascade. Understanding the molecular events following the interactions of the patient’s blood with biomaterials is crucial in the development of bone substitutes at least as effective as bone grafting.

2 – Materials and Methods

2.1 Biphasic calcium phosphate biomaterial

The biphasic calcium phosphate (BCP) biomaterial, constituted of 60% hydroxyapatite [HA, $\text{Ca}_{10}(\text{PO}_4)_6(\text{OH})_2$] and 40% β -tricalcium phosphate [β -TCP, $\beta\text{-Ca}_3(\text{PO}_4)_2$], was provided by Graftys SA (Aix-en-Provence, France). This Ca-P ceramic was obtained by sintering (1050°C for 5h) calcium-deficient apatite presenting a Ca/P ratio of 1.6 and prepared by an aqueous alkaline hydrolysis method. BCP microparticles of 80-200 μm and 200-500 μm diameter were prepared by crushing and wet sieving, then dried and made endotoxin free by heating at 250°C for 1h. After, particles were incubated in a CaCl_2 , $2\text{H}_2\text{O}$ solution, dried and sterilized by heating at 180°C for 2 hours before use.

2.2 Blood/BCP composite preparation

Blood was withdrawn from human healthy volunteers after informed consent. Blood/BCP composites were prepared in 2 mL syringes by mixing 800 mg of BCP particles of 80-200 or 200-500 μ m diameter with 700 μ L of human citrated blood. The syringes were left in an upright position to let the particles sediment and put at 37°C for different durations to allow blood coagulation and BCP microparticles/blood cell interactions. Then, a cylindrical cohesive biomaterial was pushed out. As a control, 80 μ L of a CaCl₂, 2H₂O solution were added to 700 μ L of citrated blood treated in the same way as blood/BCP composites, which resulted in blood clot (Supplemental Fig. S1). In neutralizing experiments, 0.5 μ g/mL of anti-human LBP (#AF870, Bio-technique) or 0.25 μ g/mL anti-human CD14 (#61D3, Bio-technique) antibodies have been added to the blood, and incubated 30 min. at 37°C (Supplemental Fig. S2). Then, the antibody containing blood was used to prepare the BCP/blood composites as explained above.

2.3 Implantation procedure of blood/BCP composites

The animal experiment was carried in accordance with the EU Directive 2010/63/EU for animal experiments. It received the approval of the Local Committee for Animal Use and Care (NCE/20158-262). The implants were prepared with the same procedure described above but in 1-mL syringes by mixing 100 mg of 80-200 or 200-500 μ m BCP particles with 200 μ L of human blood. The 16 NMRI nude mouse of 8-week-old (Janvier Labs) received 2 subcutaneous (SC) implants in the lower back; 8 mice were implanted with BCP 80-200 and the 8 others with BCP 200-500 blood composites. They were sacrificed 4 weeks later and the implants were retrieved for histological analyses.

2.4 Histological, second harmonic generation (SHG), and environmental scanning electronic microscopic (ESEM) analyses

SC implants were fixed in 10% buffered formalin for 24 h, sectioned in three pieces, and partially decalcified 10% (w/v) EDTA acid solution for 72h at RT. Decalcified samples were embedded in paraffin and serial sections of 4 mm were stained with hematoxylin, erythrosine, and safran (HES). Histological sections were scanned using the Vectra Polaris automated quantitative pathology imaging system (PerkinElmer). Analysis and pictures were carried out using the Phenochart software. Second harmonic generation (SHG) microscopy allows type I collagen fibers to appear in high contrast images, with no additional staining [23]. Thus, tissue sections prepared for histological study were also used for SHG microscopy on a Zeiss LSM 710 microscope. Mai Tai laser excitation wavelength was set to 880 nm and the SHG signal was detected in transmission and reflection mode.

For the environmental scanning electronic microscopy (ESEM) study, the BCP blood composites were fixed, 1h after they have been made, overnight at 4°C with a buffered 1.6% glutaraldehyde/0.1 M phosphate solution, rinsed, dehydrated in a graded ethanol series and dried at RT. Then, they were mounted on aluminum stubs with carbon tabs and sputter coated with carbon before to be analyzed using the environmental scanning electron microscope (Philips (FEI) XL40 ESEM TMP).

2.5 Protein and RNA extraction

After 24h incubation at 37°C, 4 cylinders of each composite material or 4 blood clots were pooled into 3ml of cooled lysis buffer [HEPES 50mM (pH 7.4); NaCl 150mM; EDTA 20mM (pH 8); CHAPS 1%; DTT 1mM; Protease and Phosphatase inhibitor cocktail (Thermo Scientific)]. They were let on ice for 30min with regular vortexings and centrifuged at 4°C, 8000g, 15 min. The supernatants were collected, and hemoglobin depleted using several HemoVoid™ columns (Biotech Support Group). Then, the protein concentration of these protein extracts were measured using the BCA protein assay kit (Thermo scientific), aliquoted

and stored at -20°C. When indicated, albumin was also partially removed using AlbuVoid™ depletion reagent kit (Biotech Support Group) following the manufacturer's instructions. The decrease in albumin concentration was checked on gel electrophoreses (Supplemental Fig. S3).

RNA extraction was performed using trizol (Life Technologies, Saint Aubin, France). Before quantitative PCR, RNAs were purified and concentrated with the RNA clean-up NucleoSpin® XS columns (Macherey-Nagel). RNA from 4 cylinders of the same composite material or three blood clots were necessary to get enough RNA. They were incubated for 0.5, 2 or 4h at 37°C.

2.6 Protein sample preparation, digestion and TMT labeling

For label-free experiments 200µg of protein extracts were mixed in 200µL of 100mM ammonium bicarbonate buffer. Proteins were reduced, alkylated and precipitated by addition of 10 µL of Tris (2-carboxyethyl) phosphine hydrochloride (TCEP 200 mM, 55°C, 1h), then 10 µL of iodoacetamine (375 mM, 20°C, 30 min) and 1mL cold acetone (-20°C, O/N). The samples were centrifuged (8000g, 10 min, +4°C), acetone removed and the protein pellet was dissolved in 100mM ammonium bicarbonate buffer. Proteins were then digested by 10µg of trypsin (Promega corporation) over night at 37°C, the digestion was stopped by 5% formic acid and the resulting peptide solution was dried and frozen at -20°C before LC-MS/MS analyses. All the reagents came from Sigma-aldrich®.

TMT labeling was performed according to the TMT duplex Isobaric Mass Tagging kit instructions (Thermo Scientific, # 90063). Briefly, protein extracts (100 µg) from the BCP 80-200 and BCP 200-500/blood composites were prepared and digested as above. The subsequent peptides were then respectively labeled with the TMT²-126 and TMT²-127 and then pooled before analysis.

2.7 LC-MS/MS analyses

The dried peptides were diluted into 100 μ L of H₂O/acetonitrile (80:20) containing 5% of formic acid and centrifuged (15 000g, 30 min, +4°C). Ten microliters of the resulting supernatant were analyzed using an ESI-Q Exactive Plus mass spectrometer coupled to an Ultimate 3000 RSLC Nano System (Thermo Scientific). Liquid chromatography was performed with an EASY-Spray Pepmap C18, 2 μ m, 25 cm x 75 and 100 μ m column. The flow rate was set at 0.3 μ L/min with a 5-45% gradient of solvent B (80% acetonitrile, 20% water, 0.1% formic acid) against solvent A (0.1% formic acid, 100% water) for 240 min. For MS analyses, full-scan mass spectra were measured from 350 to 1500 m/z with an AGC (Automatic Gain Control) target of 3×10^6 and a resolution of 70 K. A top 15 data-dependent method was used for MS/MS spectrum acquisition with an AGC target of 1×10^5 , a resolution of 35K and a dynamic exclusion of 40s. All MS raw data files were analyzed by Proteome Discoverer software 1.4 (Thermo Scientific) using the Sequest HT search engine against the Uniprot human database (Version 2015_2). Precursor mass tolerance was set to 10 ppm and fragment ion tolerance was 0.02 Da. Carbamidomethylation on cysteine (+57.021Da) was set as static modifications and oxidized Methionine as dynamic modification (+15.995 Da).

A decoy database search strategy was also used to estimate the false discovery rate (FDR) to ensure the reliability of the proteins identified and at least two peptides were required for matching a protein entry for its identifications.

For TMT quantitative analysis, TMT duplex (N Terminal, K) quantification method within Proteome Discoverer software was used to calculate the reporter ratios with mass tolerance ± 10 ppm. Only peptide spectra containing all reporter ions were designated as 'quantifiable spectra'. A protein ratio was expressed as a median value of the ratios for all quantifiable spectra of the peptides pertaining to that protein. The proteins with a fold change greater than 1.2 were kept for further pathway analysis.

2.8 ELISA quantification

Briefly, LBP, total CD14, NOS2, MST1, IL-12 and fibrinogen (Ozyme) were measured using sandwich ELISA technique according to the manufacturer's instructions. Detection assay is based on the horseradish peroxidase colorimetric reaction by adding TMB substrate. Absorbance was read at 450 nm immediately.

2.9 Reverse transcription and Real-time PCR

Reverse transcription was performed with 1 µg of RNA, random primers and the Superscript II/Rnase H-/Reverse transcriptase (Life Technologies). A tenfold dilution of cDNAs was used for amplification reactions. Primer sequences are listed in Supplementary Table S1. For quantitative PCR (q-PCR), final reaction volume was 10 µl using SYBR qPCR premix Ex TaqII from Takara (Ozyme), and assays were run on a StepOne Plus ABI real-time PCR machine (PerkinElmer). The expression of the selected genes was normalized to that of 36B4 housekeeping gene, and the quantification was made using the comparative CT method.

2.10 Statistical analysis

For RT-PCR and ELISA, quantifications were made in triplicates and each experiment was repeated at least 3 times. Data are expressed as mean values \pm standard deviation, and analyzed using the Mann–Whitney test. Differences were considered statistically significant at $p \leq 0.05$. For comparative proteomics analyses, a two-tailed student's t-test was used. Proteins with a p-value ≤ 0.05 and a fold change ≥ 2 (3 experiments) or ≥ 4 (one experiment), are considered deregulated and kept for further pathway analysis. Core analyses were carried out using Ingenuity IPA software (QIAGEN) in order to identify canonical pathways. The significance level of deregulated pathways was calculated using a Fisher's exact test with a threshold set at p-value = 0.05.

3 – Results

3.1 Osteogenic properties of BCP particles associated to blood clot: influence of particle size.

The observation of the BCP microparticles with a high performance stereomicroscope (Fig. 1, top), showed that except of their size, the particles had the same morphology, which was due to their method of manufacture. Indeed, they were fabricated from the same ceramic blocks (after crushing and sieving) so they had also the same global porosity of 59.2% (Hg intrusion method) in a range covering 0.1 to 10 μ m (equivalent diameter of pores). The comparative surface to volume ratio (S/V) using equivalent diameters of both populations of particles revealed that a given volume of 80-200 BCP particles presents a doubled potential surface of exchange with cells compared to 200-500 BCP particles. At a smaller scale, a given volume of 80-200 BCP particles presents the same specific surface area ($2.85 \pm 0.01\text{m}^2/\text{G}$) for exchange with fluids compared to 200-500 BCP particles. In addition, the zeta potential of bone (1 μ m powder), BCP 80-200 and BCP 200-500 particles was respectively of -75.2 mV (control); -2.1 mV and +2.0 mV, when all the suspensions were prepared in physiologic saline (pH=7.4) after previous soaking in blood (5 min, RT).

BCP 80-200 μ m or 200-500 μ m microparticles embedded into a blood clot resulted in a cohesive and moldable composite that can be easily handled (supplementary fig. S1). When these two biomaterials were subcutaneously implanted into mice for 4 weeks, the intergranular space of each resulting implant, was colonized by a very different tissue (Fig. 1, bottom). Histological examination of sections from the 80-200 μ m implants (Fig. 1A) showed that the intergranular space was colonized by woven bone tissue, characterized by osteocyte-like and giant multinucleated osteoclast-like cells embedded in a collagen matrix. Many blood vessels were also visible (on average 93 ± 40 /implant slide). The osteoblastic phenotype, as well as the mineralization of the collagen matrix have been previously characterized by

immunologic detection of the osteocalcin and Goldner staining respectively [11]. Comparatively, histological examination of the 200-500 μ m implants (Fig. 1B) revealed that the collagen matrix has a much more fibrous appearance and contained fibroblastic-like cells aligned along the collagen fibers. No ‘osteoclast-like’ cells were visible and about 10 times fewer blood vessels (9 ± 4 / implant slide on average) compared to the implants made with 80-200 μ m BCP particles. Transmission pictures of longitudinal sections (Fig. 1C, 1D) revealed that in both types of implant, the collagen matrix was more abundant on the periphery than on the inside, suggesting that tissue colonization likely evolved from the outside to the inside. This was confirmed by SHG analyses which showed that the organization of the collagen matrix of the 200-500 μ m implants (Fig. 1F) was characteristic of a fibrous tissue (more numerous and parallel collagen fibers) than that of the 80-200 μ m implants (Fig. 1E). Thus, these results confirmed [11] that after *in vivo* implantation BCP 80-200 blood composites are osteogenic whereas BCP 200-500 blood composites are mainly fibrogenic. In addition, ESEM study of these BCP blood composites allowed to observe the fibrin network (Fig. 1G, H). Fibrin fibers, adhering to the particles, were visible in the interparticle spaces. In the osteogenic BCP blood composites (80-200), a very fine fibrin network, difficult to observe was visible (Fig. 1G). Comparatively, in the fibrogenic BCP blood composites (200-500), the fibrin network was clearly visible, with larger mesh and fibers significantly thicker than in the 80-200 implants. All of these results emphasizes the importance of the vascularization and the major role of the fibrin network organization in the genesis of bone tissue [7]. Therefore, these blood/BCP microparticle composites constitute good models to identify new molecules involved in blood/BCP interactions leading to bone matrix formation. Using proteomic analyses we have next compared the plasma and total blood cell proteins profiles of BCP 80-200 and BCP 200-500 blood composites after hemoglobin removal.

3.2 Label-free comparative proteomic study of osteogenic (BCP 80-200) and fibrogenic (BCP 200-500) blood composites versus blood clot.

Using a 2-fold change threshold, as well as a significant statistical difference with a p value \leq 0.05, we found respectively 80 and 92 proteins differentially expressed between blood clot and BCP 80-200 or BCP 200-500 blood composites. Among these proteins, 41 were in common (Fig. 2A), thus 39 and 51 proteins were differentially expressed between BCP 80-200 and BCP 200-500 blood composites. These results strongly suggested that the two sizes of BCP particles stimulated protein synthesis by blood cells in very different ways.

The analyze of these two protein lists with the Ingenuity software revealed that respectively 28 and 27 canonical pathways were significantly deregulated in blood cells stimulated with 80-200 BCP or 200-500 BCP particles compared to blood clot and among them, 23 pathways were significantly more altered by the BCP 200-500 particles (see the 17 most deregulated pathways on Fig. 2B). Consistently, the complement and the coagulation system were in the first 5 most deregulated pathways. The 3 others were: the acute phase response signaling, the liver X receptor (LXR) and the farnesoid X receptor (FXR) (Fig. 2B). When the complement system and the acute phase response signaling were similarly altered, the LXR, FXR and the coagulation pathways were more strongly deregulated in blood cells in contact with BCP 200-500 rather than with BCP 80-200 particles (Fig. 2B). Owing to the wide concentration range of plasma proteins, we hypothesized that proteins abundantly expressed such as albumin (75% of the total plasma proteins) could mask less abundant proteins of interest. Therefore, we next examined the deregulated proteins and pathways after albumin depletion and low abundance plasma protein enrichment.

After albumin depletion, analysis of the significant deregulated proteins showed that 27 signaling pathways significantly changed in blood cells stimulated with BCP 80-200 particles compared to blood cells in blood clot, whereas only 6 of these pathways were significantly

deregulated with BCP 200-500 particles (see the 13 most deregulated pathways on Fig. 2C). These data obtained after low abundance protein enrichment confirmed that the acute phase response protein, as well as LXR and FXR pathways, were highly modulated in BCP blood composites but, conversely to what we observed without albumin depletion, these 3 pathways were more strongly altered by the BCP 80-200 particles (Fig. 2C). Altogether, these results indicated that the proteins involved in these 3 pathways might play a major role in the discriminating effect of the two sizes of BCP microparticles on blood cells. However, although the albumin depletion allows the enrichment of proteins present in low abundance, its depletion can also bias the results since albumin can bind a broad variety of proteins [24]. Thus, we continued our analyses in both ways, that is with and without albumin depletion.

3.3 Quantitative proteomic study of osteogenic (BCP 80-200) versus fibrogenic (BCP 200-500) blood composites using TMT labeling

To identify some proteins early involved in the osteogenic capacity of BCP 80-200 blood composites, we then compared BCP 80-200 and BCP 200-500 blood composite proteins in a quantitative proteomic study. Independently of the presence (Table 1A) or the absence of albumin (Table 1B), the 5 signaling cascades significantly deregulated when comparing the blood/BCP composites to coagulated blood (coagulation, complement, acute-phase, FXR/RXR and LXR/RXR), appeared also modified when comparing BCP 80-200 versus BCP 200-500 blood composites. Indeed they were among the 15 mostly altered pathways in both analyses as well as that of the extrinsic/intrinsic prothrombin activation and the glucocorticoid receptor signaling.

In the presence of albumin (Table 1A), the deregulation of the first 15 pathways resulted from the modification of the expression of 16 proteins (Fig. 3A). Among them, 3 keratins (KRT2,

KRT9, KRT10) whose the presence must be an artifact due to the sample preparation since these molecules are not supposed to be present in blood. In the 13 remaining proteins, 11 were overexpressed in BCP 80-200 compared to BCP 200-500 blood composites and 2 were down-regulated (Fig. 3A). The 3 fibrinogens (FGA, FGB, FGG) were the most overexpressed proteins in BCP 80-200 implants, suggesting a major involvement of fibrinogen (FGN) in the generation of woven bone or fibrous tissue *in vivo*. The 8 other up-regulated proteins were involved in lipid metabolism, extracellular matrix and insulin growth factor pathways as well as in DNA repair. The two down-regulated proteins in 80-200 BCP blood composites were complement proteins (*C4BPA*, *CIQC*).

After albumin depletion (Table 1B), the marked alteration of the acute phase response, IL-12 signaling, the production of Nitric oxide and reactive oxygen species, as well as the pattern recognition receptors pathways strongly suggested that monocytes are key players during the interactions between BCP microparticles and blood cells. Furthermore, data shown in the Table 1B suggested that the immune response, lipid metabolism as well as cytoskeletal changes were the main early biological processes governing the osteogenic properties of BCP 80-200 blood composite. Indeed, among the 36 deregulated proteins involved in the above signaling cascades (Fig. 3B), 13 were coagulation and/or acute-phase proteins, 11 belonged to the complement system, 4 were apolipoproteins, 3 were components of actin cytoskeleton and 2 from ECM signaling. Finally, one was involved in DNA repair and the last one in HGF signaling pathway. Surprisingly, 34 of these 36 proteins were overexpressed in osteogenic (BCP 80-200) compared to fibrogenic (BCP 200-500) blood composites, including *CIQC*. Conversely to what we observed in the absence of albumin depletion, fibrinogen proteins (FGB, FGG) were strongly under-expressed (not shown). The discrepancy between these two

analyses must be due to the albumin depletion, since albumin has been described to be able to interact with FGN and some complement proteins [24].

We showed previously using a transcriptomic approach that the TLR4 pathway was involved in BCP 80-200 particles induced inflammatory processes in blood cells [16]. Since FGN, which is strongly overexpressed in BCP 80-200 compared to BCP 200-500 blood composites, is a potential endogenous ligand of TLR4, we next focused on up-regulated proteins belonging to the TLR4 pathway. Figure 4 pointed out 11 proteins from the TLR4 signaling pathway which were overexpressed in osteogenic blood composites compared to fibrogenic composites namely: fibrinogens (FGA, FGB, FGG), calprotectin (S100A8/A9), complement factor H and its related protein 1 (CFH, CFHR1), apolipoprotein A1 (APOA1), LBP and its receptor CD14 (monocyte differentiation antigen CD14), and IRAK4. IRAK4 is one of the inducers of the transcription factor NF- κ B which in turn regulates the transcription of numerous cytokines, chemokines and growth factors. Among them, the hepatocyte (HGF) and the insulin growth factors (IGF) known to be trophic factors for bone [25, 26]. Respectively, three (IGFBP3, IGF1R, IGFL1) and two (HGFAC, MST1) proteins from the IGF and the HGF pathways were also up-regulated in BCP 80-200 compared to BCP 200-500 blood composites, strongly suggesting that these 2 growth factors are early involved in the osteogenesis induced by BCP 80-200 blood composites *in vivo*.

3.4 Transcriptomic validation of the overexpression of the TLR4 pathway in osteogenic (BCP 80-200) compared to fibrogenic (BCP 200-500) blood composites

Data shown in the figure 5 revealed at the gene level that the two sizes of BCP particles significantly up-regulated the TLR4 signaling pathway in blood cells, and that 80-200 were significantly more effective than 200-500 BCP microparticles. Calprotectin S100A8/A9, LBP and its specific receptor CD14, TLR4, My88 and IRAK4 genes were significantly

overexpressed in blood cells after 2h of contact with 80-200 BCP particles. This significant up-regulation lasted till 4h for S100A8/A9, CD14, TLR4, My88 and IRAK4 and was observed as early as 0.5h for the S100A8/A9, LBP, CD14, TLR4 and My88 genes. The RelA gene, coding for the subunit p65 of NF- κ B transcription factor, was also significantly overexpressed in BCP 80-200/blood composites after 2 and 4h of blood cell stimulation. Thus, in blood cells the TLR4 pathway was more solicited by the 80-200 BCP particles than by those of 200-500, which should result in higher stimulation of the transcription factor NF- κ B and its target genes.

Because the LBP protein and its receptor CD14 have a strategic position in the TLR4 pathway, we hypothesized that these 2 proteins could "switch" and direct the cells towards a synthesis of **woven bone** or fibrous tissue. Thus, we next investigated the involvement of these 2 proteins as key modulators.

3.5 Validation of the involvement of LBP and CD14 proteins in osteogenic (BCP 80-200) compared to fibrogenic (BCP 200-500) blood composites

First we confirmed by an ELISA assay that the amounts of LBP and CD14 proteins were significantly ($p \leq 0.001$) higher in osteogenic compared to fibrogenic blood composites as well as compared to blood clot (Fig. 6A).

Then, we investigated the implication of these proteins in BCP 80-200 microparticle interactions by the mean of antibodies neutralizing the LBP or CD14 (Supplemental Fig. S3). We performed a label-free comparative proteomic analysis and compared the proteomic signatures obtained with and without the antibodies (Fig. 6B). As expected, the addition of neutralizing anti- LBP antibody into the blood used to prepare BCP 80-200 blood composites resulted in a very similar signature to that obtained in the presence of anti-CD14. The presence of antibodies induced a high deregulation of the LXR and FXR/RXR pathways, IL-12 signaling and production in macrophages, clathrin-mediated endocytosis, atherosclerosis,

Fc α receptor-mediated phagocytosis in M/M, production of NO and reactive oxygen species in M/M, MSP-Ron and of BRCA1 in DNA damage response signaling pathway, but neutralized the deregulation of the cell cycle: G2/M DNA damage checkpoint pathway, induced by BCP 80-200 particles in blood cells (Fig. 6B). Therefore, the anti-LBP and anti-CD14 deeply altered numerous macrophage signaling pathways, with only minor modifications in the coagulation and the thrombin activation pathways.

We next measured the concentration of a set of proteins from the above deregulated pathways, in blood and blood/BCP composites prepared in the presence or in the absence of neutralizing anti-LBP and anti-CD14 antibodies. Data shown in the figure 6C indicated that the concentration of FGN was dramatically higher in blood clot alone compared those in the two composites and much higher (about 2 times more) in BCP 80-200 compared with BCP 200-500 blood composites. This suggested that the BCP microparticles inhibited FGN production by blood cells and the 200-500 more than the 80-200 particles. The presence of the two antibodies significantly decreased the amount of FGN in the three conditions.

Without antibodies, we observed that the quantities of NOS2 and MST1 were much higher in BCP 80-200 than in BCP 200-500 blood composites but were greater than that of blood clot. Therefore, BCP particles might induce NOS2 and MST1 synthesis by blood cells. The addition of anti-LBP and anti-CD14 resulted in a significant decrease in both proteins in the three conditions (Fig. 6C). IL-12 was detected in none of our protein extracts (not shown).

Consequently, these results let think that the overexpression of LBP and its CD14 membranous receptor induced by BCP 80-200 particles in blood monocytes, would play a major role during blood cells/BCP interactions and might switch early between induction of [woven bone](#) or fibrous tissue synthesis.

4 – Discussion

During bone reconstruction, interactions of blood with biomaterials is the first and pivotal event that influence biomaterial integration into host tissues and bone healing [3, 4, 6, 7, 22]. A number of previous works have mainly focused on the interaction between bone substitutes and osteoinductive cells [5, 27, 28] whereas the molecular mechanisms underlying blood/biomaterial interaction remain elusive. Here, we first showed that human whole blood clotted around 80-200 μ m BCP particles were able to induce ectopic woven bone formation after subcutaneous implantation in Nude mice whereas, implantation of BCP 200-500 blood composite resulted in the generation of a fibrous tissue. These results confirmed those we obtained previously using mouse blood and C57BL / 6 mice [11] and are in agreement with other studies which clearly demonstrated that different physical properties of BCP ceramics such as particle size [2, 9, 29], largely affected their efficacy in osteoinduction.

Shortly after blood-biomaterial contact, a variety of blood proteins adsorbs onto implant surfaces. The concentration, composition and conformation of this protein layer vary according to the material physicochemical properties and promote either favorable (osteogenesis) or adverse (fibrogenesis) cellular and tissue responses [3, 5, 22]. The LC-MS/MS proteomic studies showed that the fibrinogen proteins (*FGA*, *FGB*, *FGG*) were the most over-expressed proteins in osteogenic compared with fibrogenic implants. The higher concentration of FGN in blood/BCP 80-200 compared to blood/BCP 200-500 composites was confirmed by an ELISA assay. Fibrinogen (FGN) is a soluble hexameric glycoprotein consisting of three pairs of homologous peptide chains (α_2 , β_2 , γ_2), synthesized almost exclusively by hepatocytes [30, 31]. Thus, this result obtained *in vitro* with blood cells was unexpected. However, FGN is also thought to be synthesized by platelets and stored in the

platelet α -granules [32] suggesting a higher decrease in platelet activation by BCP 200-500 than by 80-200 particles. We also found that the main signaling pathways deregulated between the osteogenic and fibrogenic composites were involved in the following biological processes: coagulation, acute phase inflammation, innate immune response, lipid metabolism and cytoskeleton changes. In addition, our results strongly suggested that blood monocytes would be the key players, which is in agreement with our previous study showing that BCP 80-200 microparticles induced monocyte proliferation in BCP/blood composites [16]. Our results are also consistent with a major involvement of FGN. Indeed, FGN has long been associated with multiple biological functions: main actors of clot formation, positive acute phase protein, modulator of immune cell responses and extracellular matrix (ECM) interactions through growth factor, integrin and cytokine binding [30, 31], actor of atherosclerosis [33], as well as bone healing [34, 35]. Moreover, FNG has been described to promote the monocyte adhesion to biomaterial surface [36].

The few studies dealing with protein adsorption onto BCP have focused on the exposure of BCP to single protein solution [37, 38] or mixtures of some known molecules [3, 21]. But, blood is a multicomponent protein solution where the different kinds of proteins would competitively adhere to the biomaterial surface according to the “Vroman effect” [22]. The adsorption of blood proteins onto biomaterial surface induces the activation of the coagulation cascade (fibrin generation) and complement system [3, 5]. The 3D network of fibrin and structural proteins of the clot serve as physical scaffolds to support leukocyte adhesion and migration, activating their secretion of inflammatory cytokines and growth factors. Then, osteoinduction will be largely affected by [the density and organization of the fibrin network \[7\]](#), and more generally by the blood clot structure [4, 8]. Increasing concentrations of FNG in fibrin clots has been reported to increase the stiffness of the gel [39]. Therefore, a change in

FNG concentration should modify the blood clot mechanoproperties, which in turn might modulate blood/BCP composite osteoactivity. This hypothesis is strengthened by the study from Kim et al. [34] which demonstrated in a rabbit calvarial defect model that FNG adsorbed on BCP microparticles improved bone healing in a dose-dependent manner. Monocytes/macrophages (M/M) are known to respond to different stiffness of growth surfaces mainly through their membrane integrin receptor CD11b/CD18 (Mac-1) [30, 40]. We did not detect this receptor during our proteomic study. Nevertheless, it is possible that it participates in the conversion of physical cues from the extracellular microenvironment into biochemical signals in BCP/blood composites. However, according to Oliveira et al. [35], this receptor would not play an important role in the interaction of monocytes with immobilized FGN. Recently, Gruber E et al. [41] demonstrated that the substrate stiffness could affect M/M response through the stimulation of their Toll-like receptor 4 (TLR4) but, whether M/M mechano-signals are transduced via integrins and/or other mechano-sensors remains to be determined. FNG being a potential endogenous ligand of TLR4 (or an “alarmin”) [18, 42], we search and found several upregulated proteins involved in the TLR4 signaling pathway. Indeed, our proteomic and transcriptomic studies showed that in BCP/blood composites, the TLR4 pathway is strongly up-regulated in osteogenic compared to fibrogenic composites and involved a MyD88-dependent nuclear factor- κ B activation. The TLR4 cascade might be stimulated mainly by FGN, but also by calprotectin which is another “alarmin“ [18]. Indeed, both have been described to activate TLR4 through MyD88 and NF- κ B [19, 43]. In addition, we showed that BCP particles induced blood cells to synthesized two (*HGFAC*, *MST1*) and three (*IGFBP3*, *IGF1*, *IGF1R*) proteins involved respectively in the HGF [25] and the IGF [26] osteogenic pathways presumably via the TLR4 signaling cascade (Fig.7).

To the best of our knowledge a direct binding of FGN to TLR4 has never been demonstrated. Thus, one can assume that the TLR4 pathway activation by the FGN is either direct, or

indirect, or both. About 16% of the FGN circulate as lipoprotein particles (FALPs) constituted of apolipoprotein A-1 (*APOA1*), complement factor H-related proteins (*CFHR*), lipopolysaccharide-binding protein (*LBP*) and phospholipids [44]. As all these proteins were overexpressed in osteogenic compared to fibrogenic BCP/blood composites, this strongly suggests that the FGN might, at least in part, activate TLR4 in the form of FALP via the LBP. The LBP and its receptor CD14 were originally discovered as proteins necessary for cellular response to lipopolysaccharides (LPS) from Gram negative bacteria. As FGN has been described to activate a TLR4 signaling cascade similar to that of LPS [19, 33], the LBP and CD14 proteins must play an important role in FGN-induced TLR4 pathway. LBP is a glycoprotein initially known as a modulator of the innate host defense, with a dual role depending on its relatively high or low concentrations [45, 46]. LBP, like FGN, is an acute-phase protein mainly synthesized in hepatocytes which can be also produced by non-hepatic cells, including M/M [47]. However in M/M, LBP gene expression is not induced in response to pro-inflammatory cytokines, but is an LXR target that promotes macrophages survival [47]. This data is in agreement with our results since the LXR/RXR cascade was one of the most deregulated pathways between the two kinds of BCP/blood composites. CD14 for its part, is the LBP receptor and it exists in two forms: as a PRR, made mostly by M/M and expressed on the surface of various cells, including M/M as well as polymorphonuclear neutrophils, and in a soluble (sCD14) state secreted by monocytes as an acute-phase protein [48]. The LBP and/or CD14 proteins have been shown to be involved in nearly all the signaling cascades significantly deregulated between the osteogenic and fibrogenic implants [45-50]. In our study, blocking LBP or CD14 with neutralizing antibodies resulted in the same and deep changes in the signaling pathway signaling of BCP 80-200 blood composites and in a marked decreased in the concentration of FGN, NOS2 and MST1, confirming an early and pivotal role of the LBP and CD14 proteins in FGN-induced TLR4 in blood/BCP microparticle

interactions, further regulating osteogenic or fibrogenic activity of these composites *in vivo* (Fig.7).

5 – Conclusions

The present findings provide an insight into the proteins and the deregulated signaling pathways, involved during blood/BCP particle interactions. By the mean of LC-MS/MS proteomic studies performed *in vitro* and in 3D in osteogenic and fibrogenic BCP blood composites, we showed that BCP-induced osteogenesis is associated with the overexpression of fibrinogen (FGN) and calprotectin which are two “alarmins”. We also found a strong upregulation of the TLR4 signaling cascade mediated through LBP/CD14-Myd88 and NF- κ B, leading to an early stimulation of at least two osteogenic pathways namely IGF [26] and HGF [25]. We highlighted the key role of the LBP/CD14 proteins in the TLR4 activation of blood cells by BCP particles. However, further *in vivo* studies are necessary to evaluate their real impact on the osteoinduction properties of blood/BCP composites. In addition, FGN being able to modulate blood composite stiffness, we propose that different FNG concentrations modify the blood clot mechanoproperties, which in turn modulate blood/BCP composite osteoactivity through TLR4 signaling. The discovery of molecular players involved in blood/biomaterial mechanobiology will allow to improve bone reconstruction.

Statement of data availability

All scientific data related to this article are available on request.

Acknowledgements and funding

The authors are very grateful to Graftys Sarl (Aix en Provence, France) for supplying BCP microparticles and to Dr. E. VERRON for giving us access to the CEMHTI electron microscopy laboratory (UPR 3079 CNRS, Orléans, France). This work was supported by funding from the “Fondation des gueules cassées” (grant N° 30-2018).

References

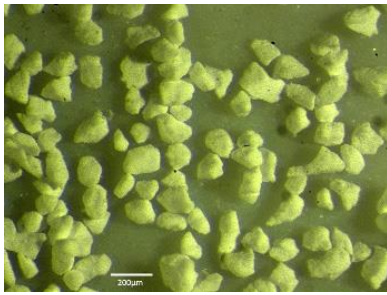
- [1] C. Laurencin, Y. Khan, S.F. El-Amin, Bone graft substitutes, *Expert Rev Med Devices* 3(1) (2006) 49-57.
- [2] J.M. Bouler, P. Pilet, O. Gauthier, E. Verron, Biphasic calcium phosphate ceramics for bone reconstruction: A review of biological response, *Acta Biomater* 53 (2017) 1-12.
- [3] S. Sapatnekar, K.M. Kieswetter, K. Merritt, J.M. Anderson, L. Cahalan, M. Verhoeven, M. Hendriks, B. Fouache, P. Cahalan, Blood-biomaterial interactions in a flow system in the presence of bacteria: effect of protein adsorption, *J Biomed Mater Res* 29(2) (1995) 247-56.
- [4] H.T. Shiu, B. Goss, C. Lutton, R. Crawford, Y. Xiao, Formation of blood clot on biomaterial implants influences bone healing, *Tissue Eng Part B Rev* 20(6) (2014) 697-712.
- [5] B.S. Kopf, A. Schipanski, M. Rottmar, S. Berner, K. Maniura-Weber, Enhanced differentiation of human osteoblasts on Ti surfaces pre-treated with human whole blood, *Acta Biomater* 19 (2015) 180-90.
- [6] J. Yang, Y. Zhou, F. Wei, Y. Xiao, Blood clot formed on rough titanium surface induces early cell recruitment, *Clin Oral Implants Res* 27(8) (2016) 1031-8.
- [7] J.E. Davies, Understanding peri-implant endosseous healing, *J Dent Educ* 67(8) (2003) 932-49 (Re-issued in 2005).
- [8] F. Wei, G. Liu, Y. Guo, R. Crawford, Z. Chen, Y. Xiao, Blood prefabricated hydroxyapatite/tricalcium phosphate induces ectopic vascularized bone formation via modulating the osteoimmune environment, *Biomater Sci* 6(8) (2018) 2156-2171.
- [9] O. Malard, J.M. Bouler, J. Guicheux, D. Heymann, P. Pilet, C. Coquard, G. Daculsi, Influence of biphasic calcium phosphate granulometry on bone ingrowth, ceramic resorption, and inflammatory reactions: preliminary in vitro and in vivo study, *J Biomed Mater Res* 46(1) (1999) 103-11.
- [10] R.Z. LeGeros, Calcium phosphate-based osteoinductive materials, *Chem Rev* 108(11) (2008) 4742-53.
- [11] T. Balaguer, F. Boukhechba, A. Clave, S. Bouvet-Gerbettaz, C. Trojani, J.F. Michiels, J.P. Laugier, J.M. Bouler, G.F. Carle, J.C. Scimeca, N. Rochet, Biphasic calcium phosphate microparticles for bone formation: benefits of combination with blood clot, *Tissue Eng Part A* 16(11) (2010) 3495-505.
- [12] A.J. Paul, D. Momier, F. Boukhechba, J.F. Michiels, P. Lagadec, N. Rochet, Effect of G-CSF on the osteoinductive property of a BCP/blood clot composite, *J Biomed Mater Res A* 103(9) (2015) 2830-8.
- [13] T. Balaguer, B.H. Fellah, F. Boukhechba, M. Traverson, X. Mouska, D. Ambrosetti, B. Dadone, J.F. Michiels, E.Z. Amri, C. Trojani, J.M. Bouler, O. Gauthier, N. Rochet, Combination of blood and biphasic calcium phosphate microparticles for the reconstruction of large bone defects in dog: A pilot study, *J Biomed Mater Res A* 106(7) (2018) 1842-1850.
- [14] A.O. Ransford, T. Morley, M.A. Edgar, P. Webb, N. Passuti, D. Chopin, C. Morin, F. Michel, C. Garin, D. Pries, Synthetic porous ceramic compared with autograft in scoliosis surgery. A prospective, randomized study of 341 patients, *J Bone Joint Surg Br* 80(1) (1998) 13-8.
- [15] R. Cavagna, G. Daculsi, J.M. Bouler, Macroporous calcium phosphate ceramic: a prospective study of 106 cases in lumbar spinal fusion, *J Long Term Eff Med Implants* 9(4) (1999) 403-12.
- [16] P. Lagadec, T. Balaguer, F. Boukhechba, G. Michel, S. Bouvet-Gerbettaz, J.M. Bouler, J.C. Scimeca, N. Rochet, Calcium supplementation decreases BCP-induced inflammatory processes in blood cells through the NLRP3 inflammasome down-regulation, *Acta Biomater* 57 (2017) 462-471.

- [17] T. Kawai, S. Akira, The role of pattern-recognition receptors in innate immunity: update on Toll-like receptors, *Nat Immunol* 11(5) (2010) 373-84.
- [18] C. Erridge, Endogenous ligands of TLR2 and TLR4: agonists or assistants?, *J Leukoc Biol* 87(6) (2010) 989-99.
- [19] S.T. Smiley, J.A. King, W.W. Hancock, Fibrinogen stimulates macrophage chemokine secretion through toll-like receptor 4, *J Immunol* 167(5) (2001) 2887-94.
- [20] M.E. Bianchi, DAMPs, PAMPs and alarmins: all we need to know about danger, *J Leukoc Biol* 81(1) (2007) 1-5.
- [21] M.M. Ouberai, K. Xu, M.E. Welland, Effect of the interplay between protein and surface on the properties of adsorbed protein layers, *Biomaterials* 35(24) (2014) 6157-63.
- [22] F. Romero-Gavilan, N.C. Gomes, J. Rodenas, A. Sanchez, M. Azkargorta, I. Iloro, F. Elortza, I. Garcia Arnaez, M. Gurruchaga, I. Goni, J. Suay, Proteome analysis of human serum proteins adsorbed onto different titanium surfaces used in dental implants, *Biofouling* 33(1) (2017) 98-111.
- [23] A. Cipitria, W. Wagermaier, P. Zaslansky, H. Schell, J.C. Reichert, P. Fratzl, D.W. Hutmacher, G.N. Duda, BMP delivery complements the guiding effect of scaffold architecture without altering bone microstructure in critical-sized long bone defects: A multiscale analysis, *Acta Biomater* 23 (2015) 282-294.
- [24] M. Zhou, D.A. Lucas, K.C. Chan, H.J. Issaq, E.F. Petricoin, 3rd, L.A. Liotta, T.D. Veenstra, T.P. Conrads, An investigation into the human serum "interactome", *Electrophoresis* 25(9) (2004) 1289-98.
- [25] R.N. Frisch, K.M. Curtis, K.K. Aenlle, G.A. Howard, Hepatocyte growth factor and alternative splice variants - expression, regulation and implications in osteogenesis and bone health and repair, *Expert Opin Ther Targets* 20(9) (2016) 1087-98.
- [26] R.C. Lindsey, C.H. Rundle, S. Mohan, Role of IGF1 and EFN-EPH signaling in skeletal metabolism, *J Mol Endocrinol* 61(1) (2018) T87-T102.
- [27] W. Thein-Han, J. Liu, H.H. Xu, Calcium phosphate cement with biofunctional agents and stem cell seeding for dental and craniofacial bone repair, *Dent Mater* 28(10) (2012) 1059-70.
- [28] Aniket, R. Reid, B. Hall, I. Marriott, A. El-Ghannam, Early osteoblast responses to orthopedic implants: Synergy of surface roughness and chemistry of bioactive ceramic coating, *J Biomed Mater Res A* 103(6) (2015) 1961-73.
- [29] O. Gauthier, J.M. Bouler, P. Weiss, J. Bosco, E. Aguado, G. Daculsi, Short-term effects of mineral particle sizes on cellular degradation activity after implantation of injectable calcium phosphate biomaterials and the consequences for bone substitution, *Bone* 25(2 Suppl) (1999) 71S-74S.
- [30] M.W. Mosesson, Fibrinogen and fibrin structure and functions, *J Thromb Haemost* 3(8) (2005) 1894-904.
- [31] R. Vilar, R.J. Fish, A. Casini, M. Neerman-Arbez, Fibrin(ogen) in human disease: both friend and foe, *Haematologica* 105(2) (2020) 284-296.
- [32] F. Belloc, E. Heilmann, R. Combrie, M.R. Boisseau, A.T. Nurden, Protein synthesis and storage in human platelets: a defective storage of fibrinogen in platelets in Glanzmann's thrombasthenia, *Biochim Biophys Acta* 925(2) (1987) 218-25.
- [33] C.P. Hodgkinson, K. Patel, S. Ye, Functional Toll-like receptor 4 mutations modulate the response to fibrinogen, *Thromb Haemost* 100(2) (2008) 301-7.
- [34] B.S. Kim, J. Lee, Enhanced bone healing by improved fibrin-clot formation via fibrinogen adsorption on biphasic calcium phosphate granules, *Clin Oral Implants Res* 26(10) (2015) 1203-10.

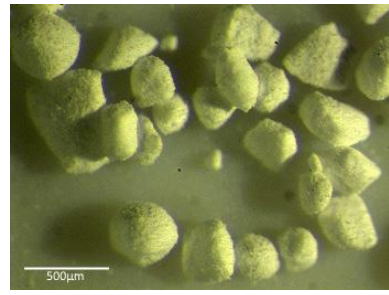
- [35] M.I. Oliveira, M.L. Pinto, R.M. Goncalves, M.C.L. Martins, S.G. Santos, M.A. Barbosa, Adsorbed Fibrinogen stimulates TLR-4 on monocytes and induces BMP-2 expression, *Acta Biomater* 49 (2017) 296-305.
- [36] T.A. Horbett, Fibrinogen adsorption to biomaterials, *J Biomed Mater Res A* 106(10) (2018) 2777-2788.
- [37] K. Cai, M. Frant, J. Bossert, G. Hildebrand, K. Liefeth, K.D. Jandt, Surface functionalized titanium thin films: zeta-potential, protein adsorption and cell proliferation, *Colloids Surf B Biointerfaces* 50(1) (2006) 1-8.
- [38] K. Xu, M.M. Ouberai, M.E. Welland, A comprehensive study of lysozyme adsorption using dual polarization interferometry and quartz crystal microbalance with dissipation, *Biomaterials* 34(5) (2013) 1461-70.
- [39] W. Ho, B. Tawil, J.C. Dunn, B.M. Wu, The behavior of human mesenchymal stem cells in 3D fibrin clots: dependence on fibrinogen concentration and clot structure, *Tissue Eng* 12(6) (2006) 1587-95.
- [40] J.Y. Hsieh, M.T. Keating, T.D. Smith, V.S. Meli, E.L. Botvinick, W.F. Liu, Matrix crosslinking enhances macrophage adhesion, migration, and inflammatory activation, *APL Bioeng* 3(1) (2019) 016103.
- [41] E. Gruber, C. Heyward, J. Cameron, C. Leifer, Toll-like receptor signaling in macrophages is regulated by extracellular substrate stiffness and Rho-associated coiled-coil kinase (ROCK1/2), *Int Immunol* 30(6) (2018) 267-278.
- [42] E. Al-ofi, S.B. Coffelt, D.O. Anumba, Fibrinogen, an endogenous ligand of Toll-like receptor 4, activates monocytes in pre-eclamptic patients, *J Reprod Immunol* 103 (2014) 23-8.
- [43] J.C. Simard, A. Cesaro, J. Chapeton-Montes, M. Tardif, F. Antoine, D. Girard, P.A. Tessier, S100A8 and S100A9 induce cytokine expression and regulate the NLRP3 inflammasome via ROS-dependent activation of NF-kappaB(1.), *PLoS One* 8(8) (2013) e72138.
- [44] C.T. Park, S.D. Wright, Fibrinogen is a component of a novel lipoprotein particle: factor H-related protein (FHRP)-associated lipoprotein particle (FALP), *Blood* 95(1) (2000) 198-204.
- [45] R.R. Schumann, Old and new findings on lipopolysaccharide-binding protein: a soluble pattern-recognition molecule, *Biochem Soc Trans* 39(4) (2011) 989-93.
- [46] M. Triantafilou, K. Triantafilou, Lipopolysaccharide recognition: CD14, TLRs and the LPS-activation cluster, *Trends Immunol* 23(6) (2002) 301-4.
- [47] T. Sallam, A. Ito, X. Rong, J. Kim, C. van Stijn, B.T. Chamberlain, M.E. Jung, L.C. Chao, M. Jones, T. Gilliland, X. Wu, G.L. Su, R.K. Tangirala, P. Tontonoz, C. Hong, The macrophage LBP gene is an LXR target that promotes macrophage survival and atherosclerosis, *J Lipid Res* 55(6) (2014) 1120-30.
- [48] S. Bas, B.R. Gauthier, U. Spenato, S. Stingelin, C. Gabay, CD14 is an acute-phase protein, *J Immunol* 172(7) (2004) 4470-9.
- [49] H.M. Liu, J.F. Liao, T.Y. Lee, Farnesoid X receptor agonist GW4064 ameliorates lipopolysaccharide-induced ileocolitis through TLR4/MyD88 pathway related mitochondrial dysfunction in mice, *Biochem Biophys Res Commun* 490(3) (2017) 841-848.
- [50] D.S. Kabanov, O.Y. Vwedenskaya, M.A. Fokina, E.M. Morozova, S.V. Grachev, I.R. Prokhorenko, Impact of CD14 on Reactive Oxygen Species Production from Human Leukocytes Primed by Escherichia coli Lipopolysaccharides, *Oxid Med Cell Longev* 2019 (2019) 6043245.

Fig. 1

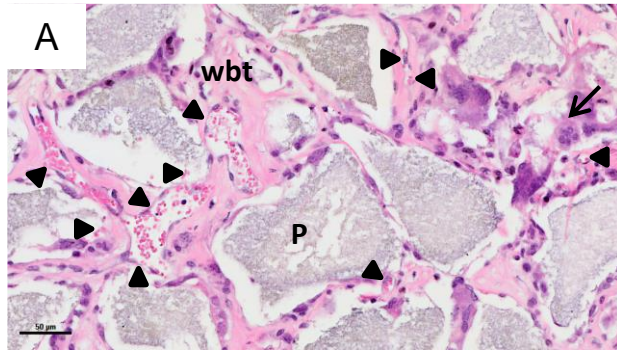
80-200 BCP microparticles



200-500 BCP microparticles



BCP 80-200 blood composite



BCP 200-500 blood composite

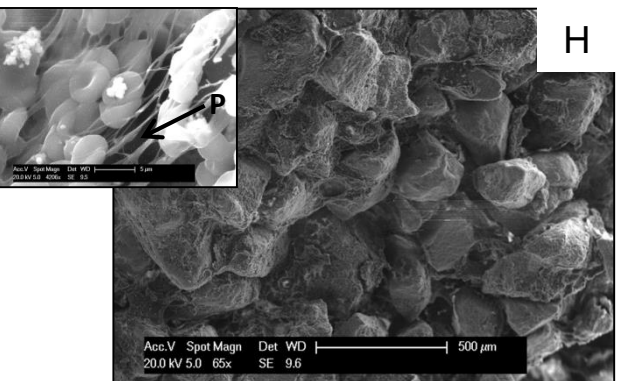
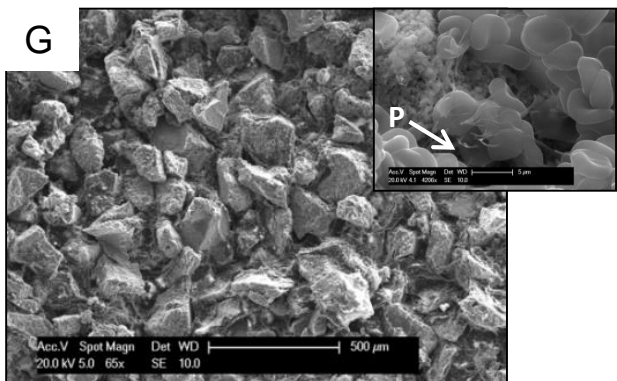
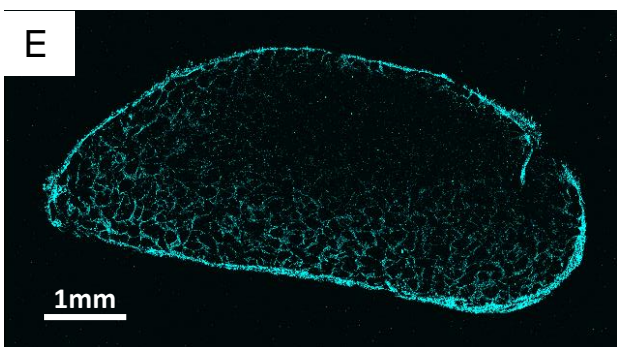
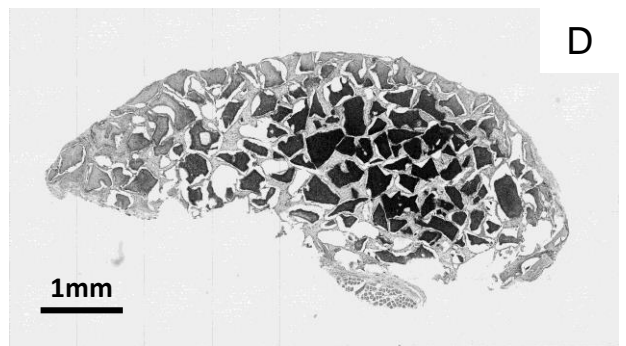
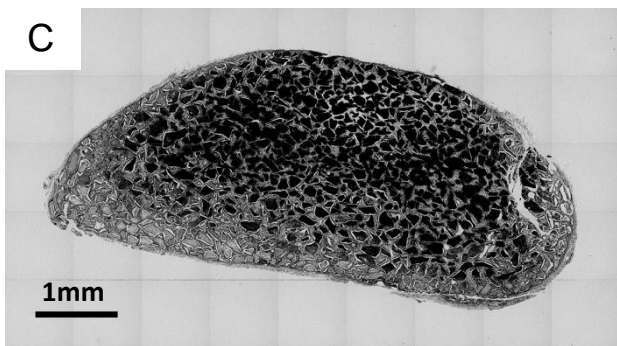
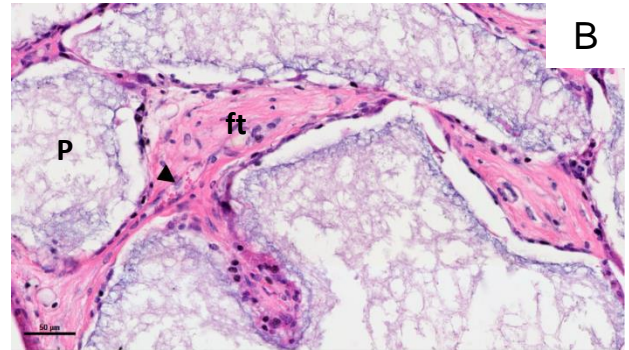
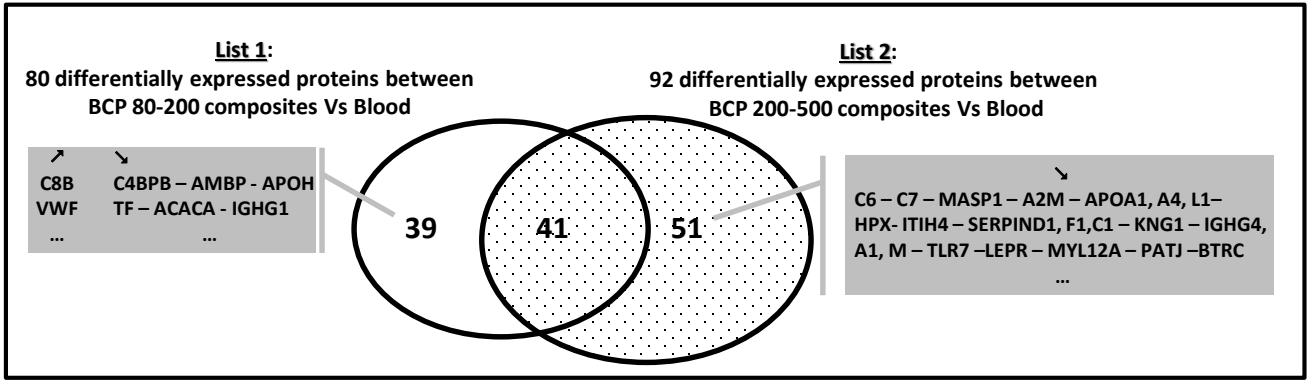
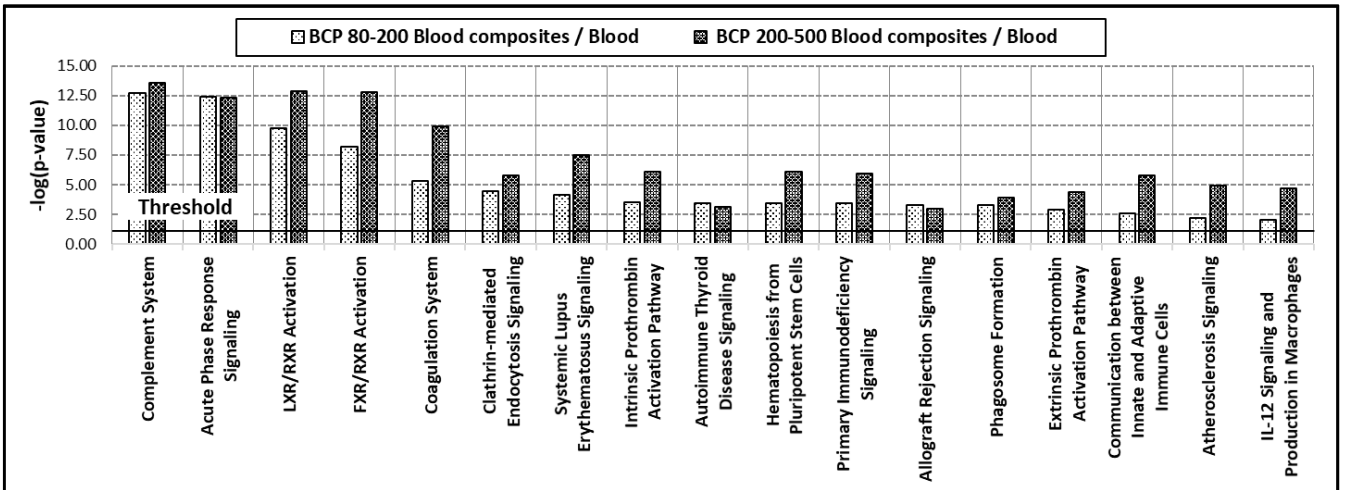


Fig. 2

A



B



C

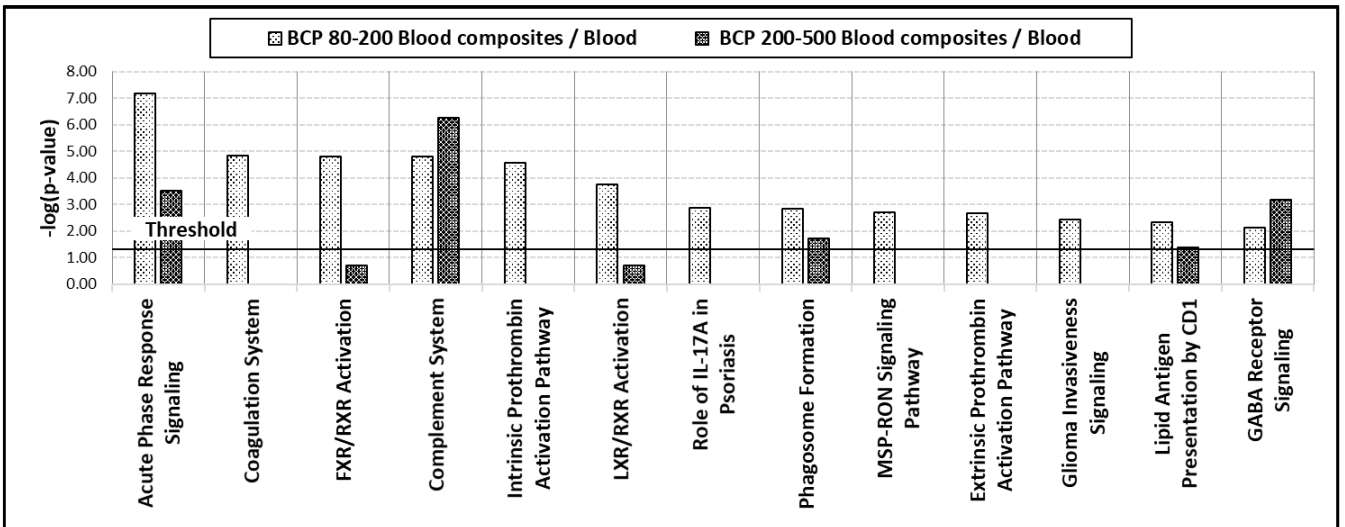
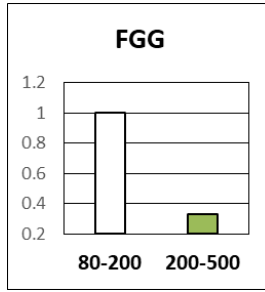
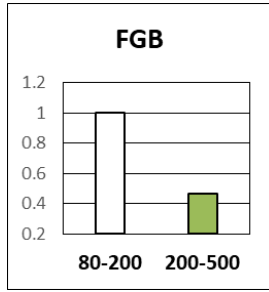
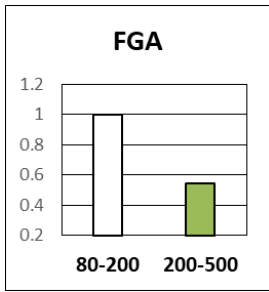
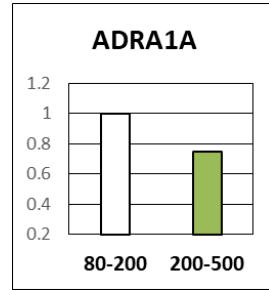
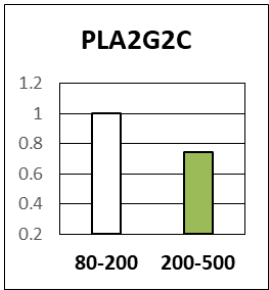


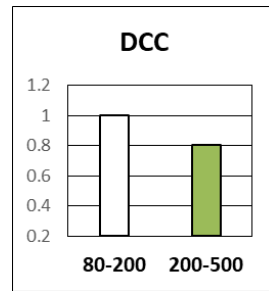
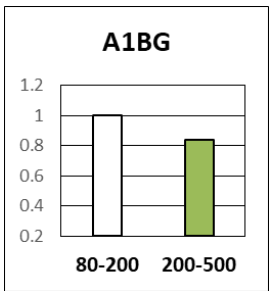
Fig. 3A



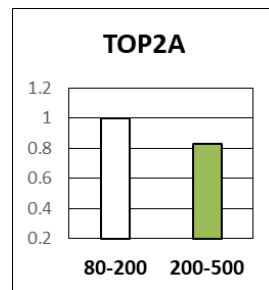
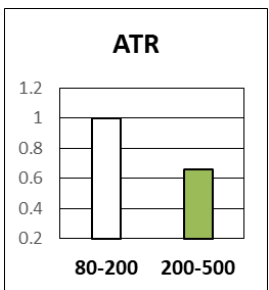
Coagulation and
Acute-phase proteins



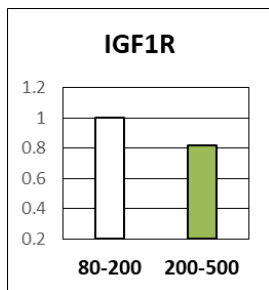
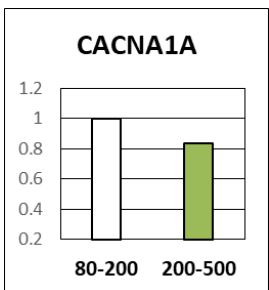
Lipid metabolism



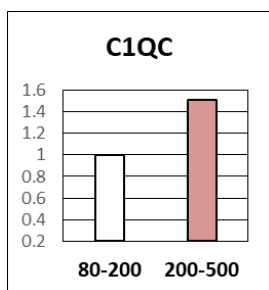
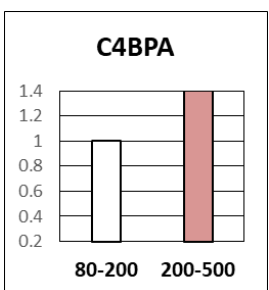
ECM signaling



DNA repair

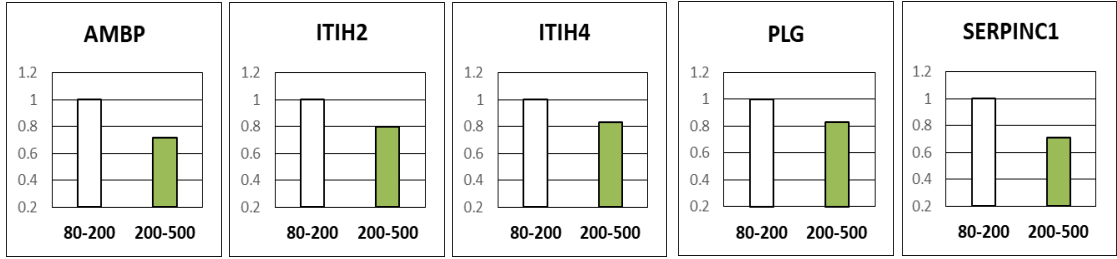
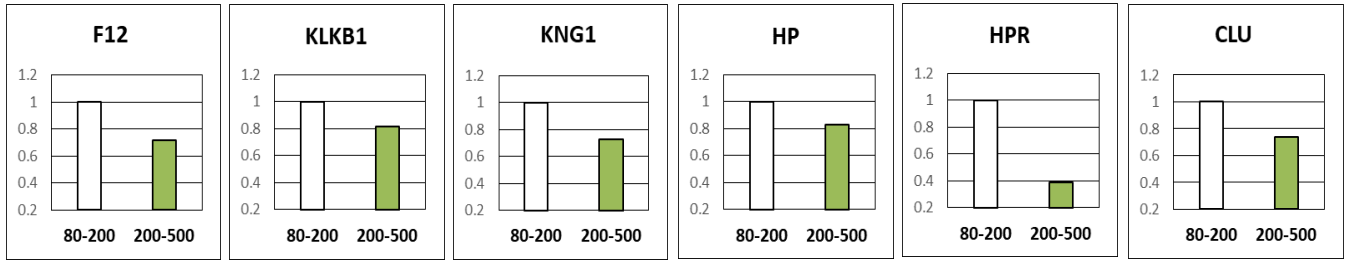


insulin signaling

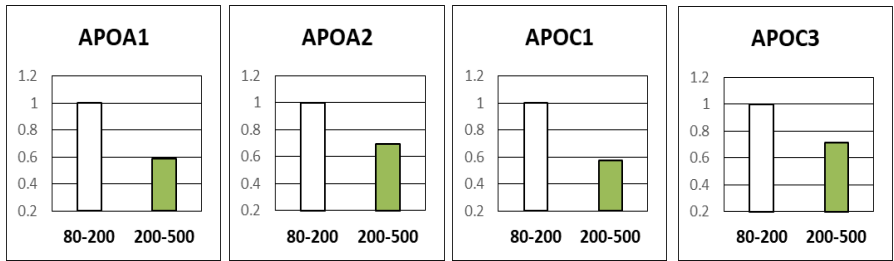


Complement system

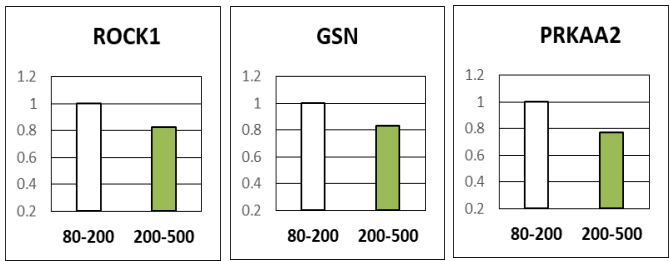
Fig. 3B



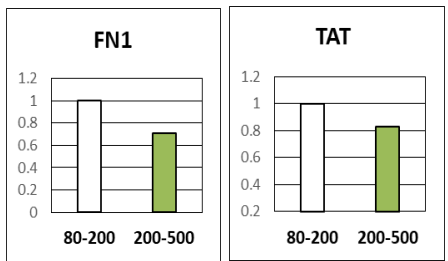
Coagulation and Acute-phase proteins



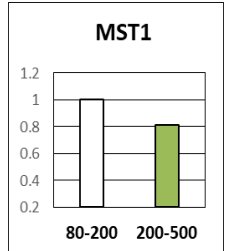
Lipid metabolism



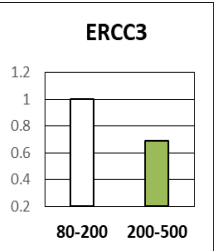
Actin cytoskeleton



ECM signaling



HGF signaling

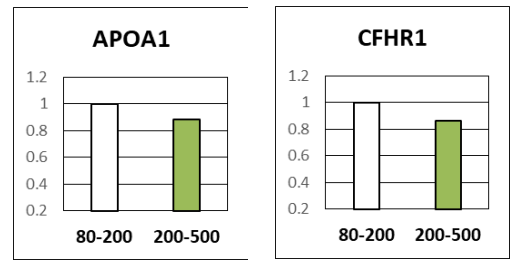
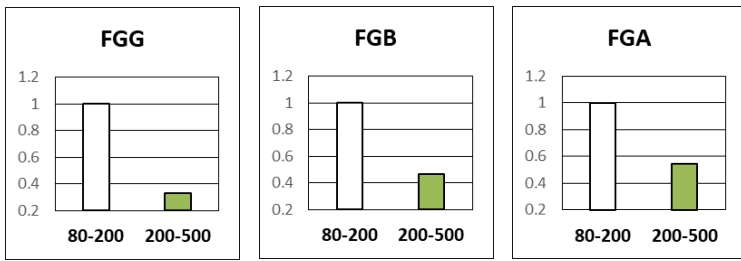


DNA repair

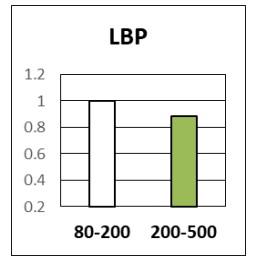
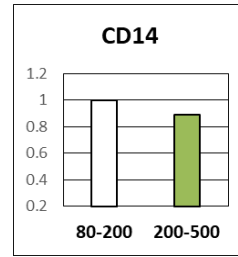
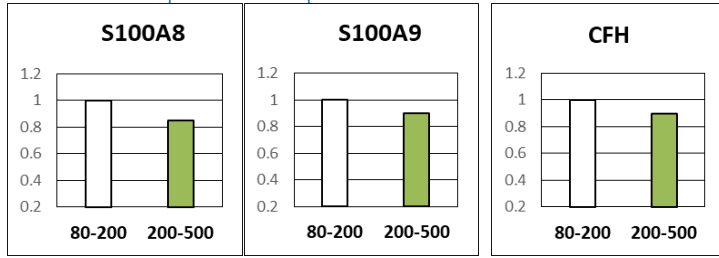
Fig. 4

TLR4 potential activators

LBP potential ligands

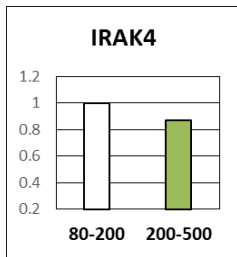


calprotectin



MyD88

IRAK4/IRAK2
(TRAF 6)



NF- κ B

Nucleus

IGF Pathway

HGF Pathway

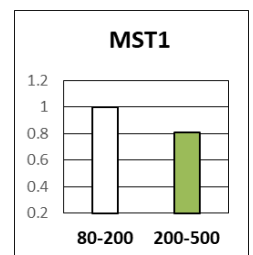
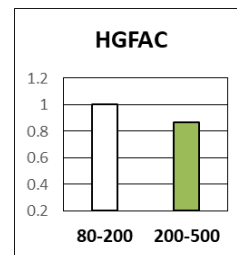
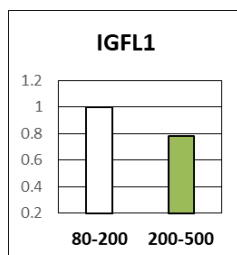
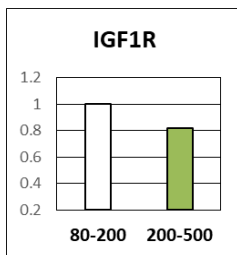
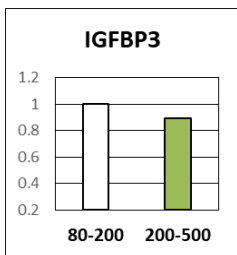


Fig. 5

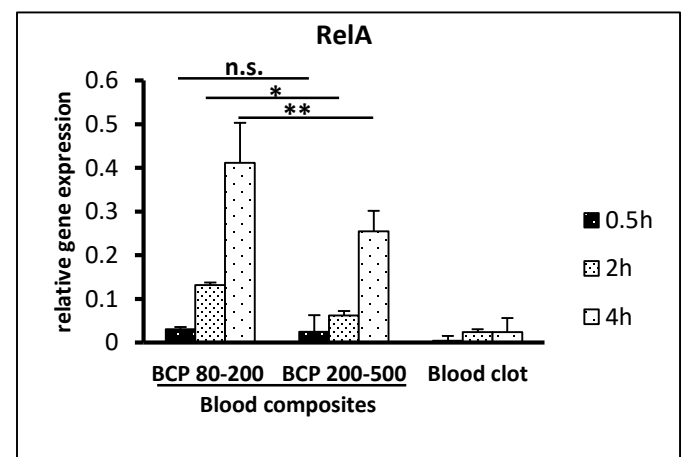
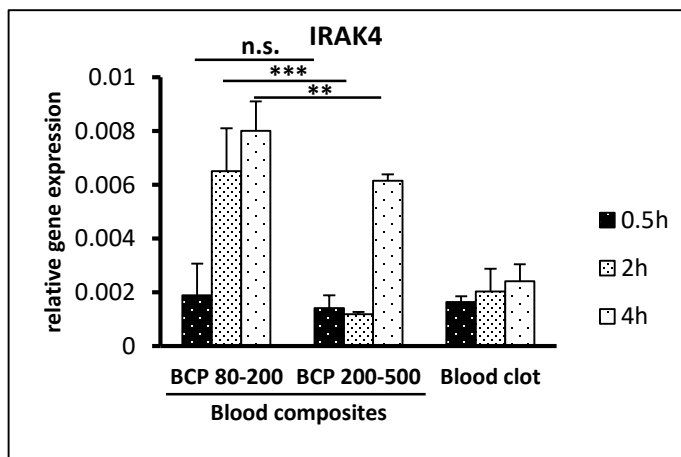
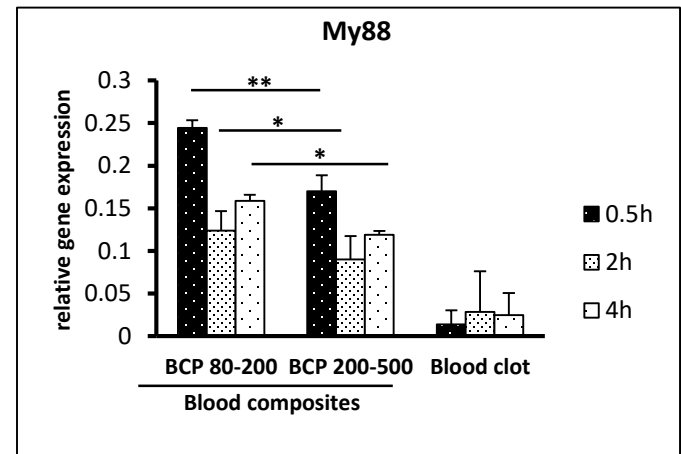
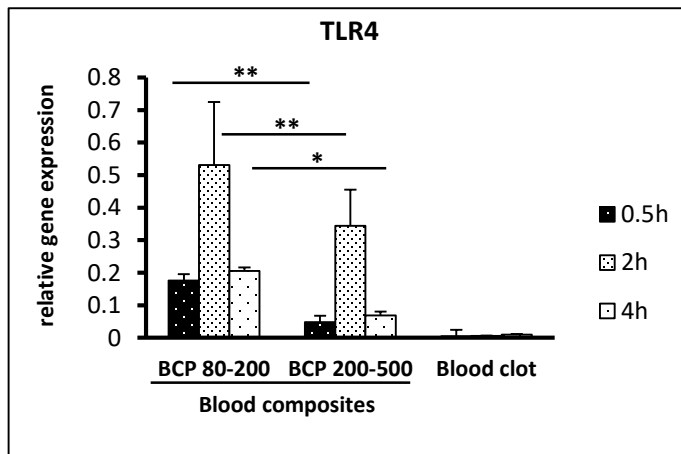
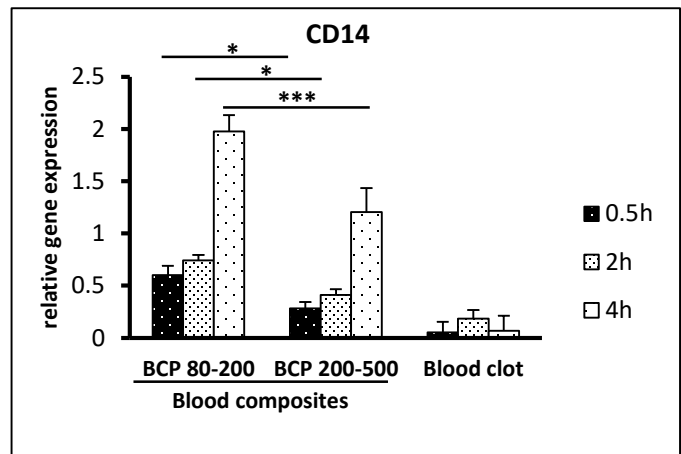
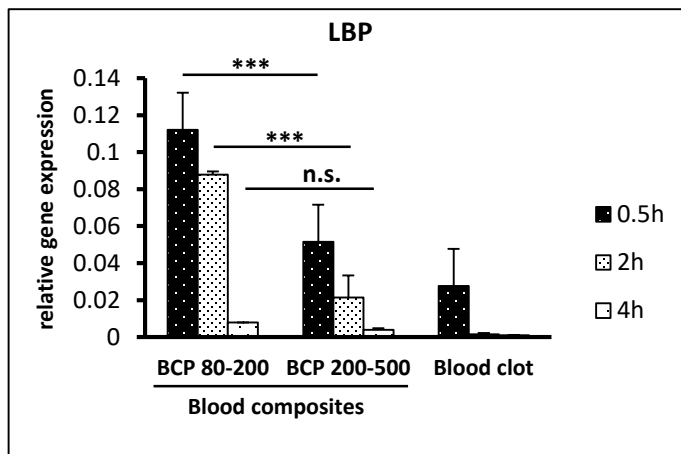
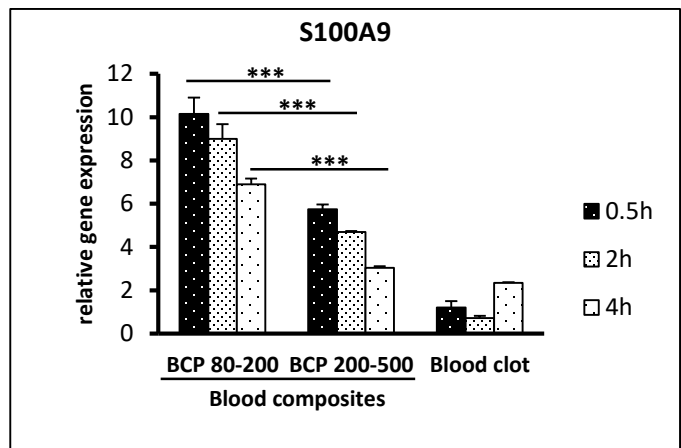
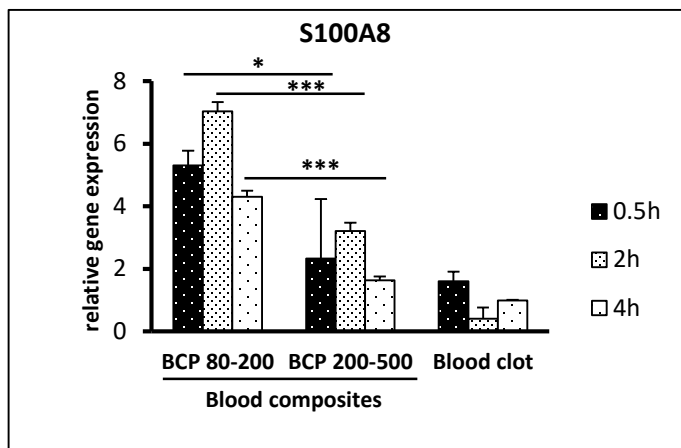
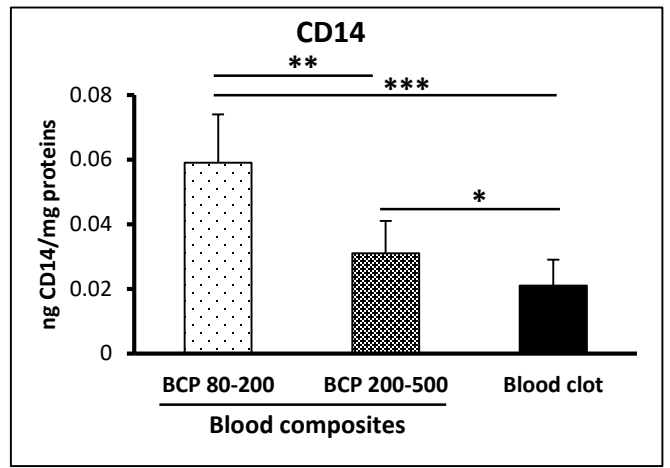
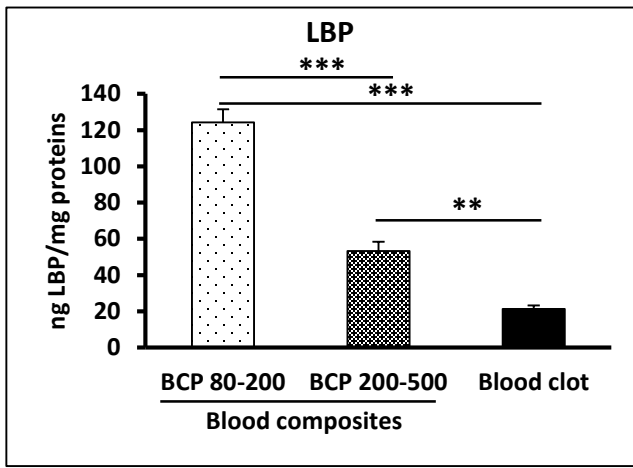
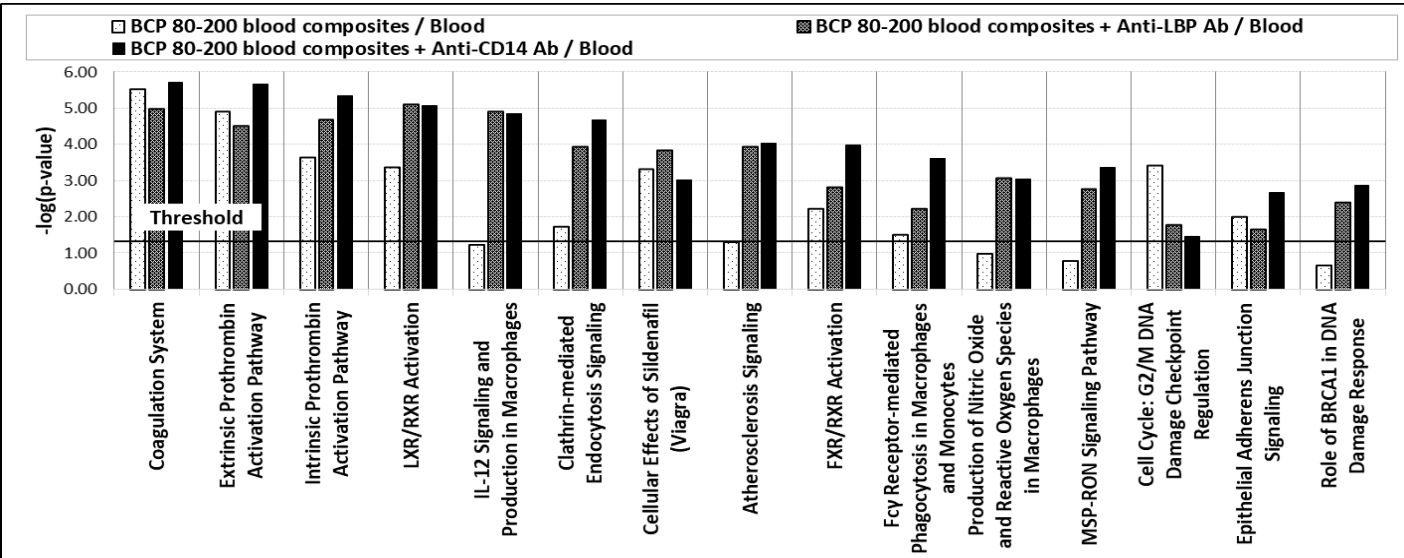


Fig. 6

A



B



C

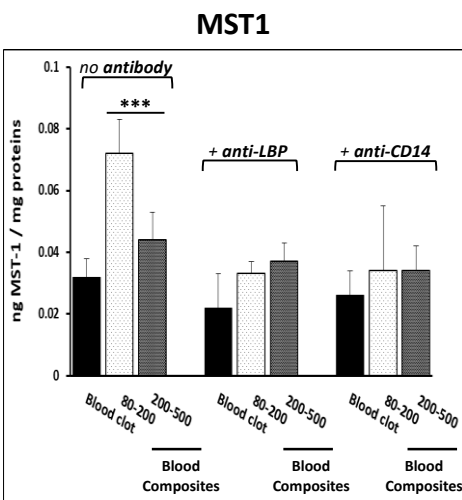
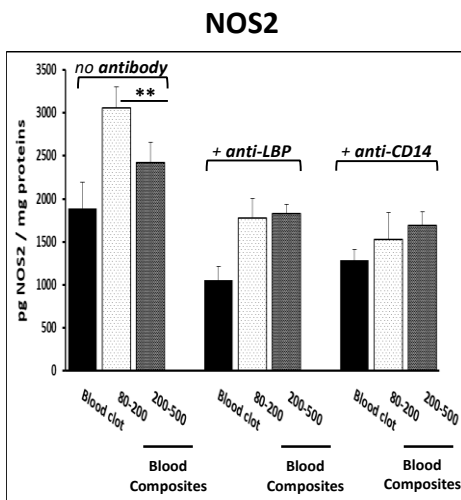
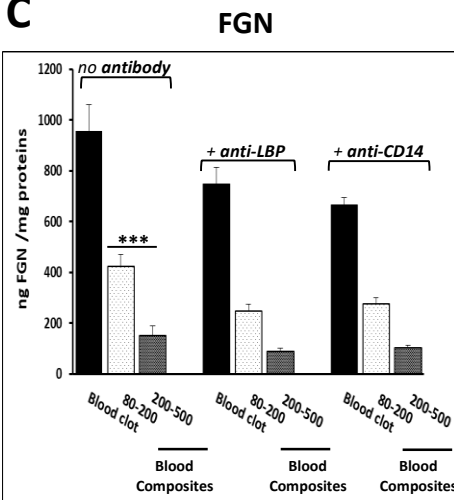


Fig. 7

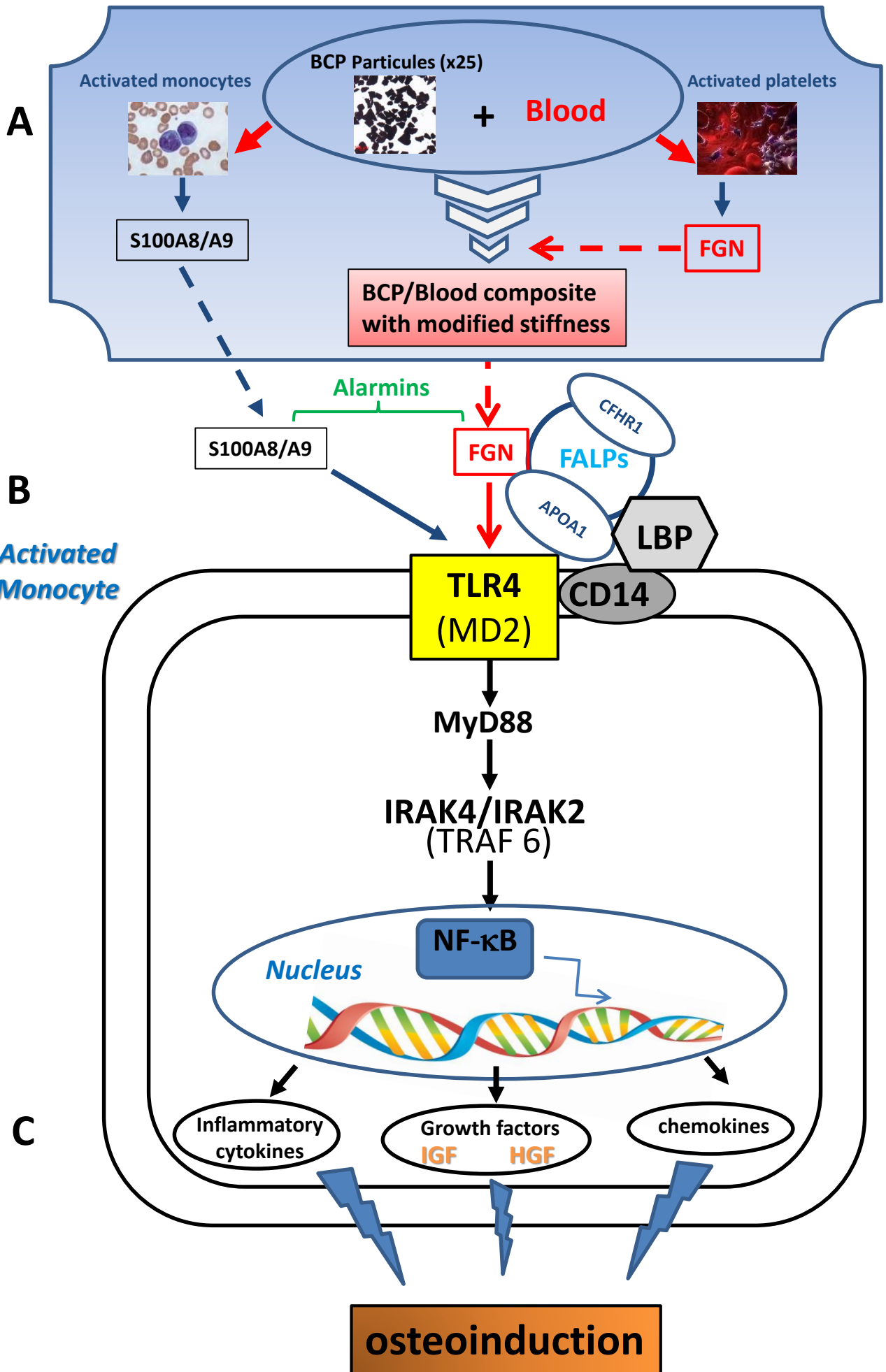


Table 1A

The top 15 differentially deregulated pathways and related proteins in BCP 80-200 versus BCP 200-500 blood composites after TMT labeling

© 2000-2019 QIAGEN. All rights reserved.

| | Ingenuity Canonical Pathways | -log(p-value) | Ratio | Molecules |
|-----------|---|----------------------|--------------|-----------------------|
| 1 | Extrinsic Prothrombin Activation Pathway | 4.94 | 0.188 | FGB,FGA,FGG |
| 2 | Coagulation System | 3.89 | 0.0857 | FGB,FGA,FGG |
| 3 | Intrinsic Prothrombin Activation Pathway | 3.65 | 0.0714 | FGB,FGA,FGG |
| 4 | Acute Phase Response Signaling | 2.82 | 0.0227 | C4BPA,FGB,FGA,FGG |
| 5 | Complement System | 2.31 | 0.0541 | C4BPA,C1QC |
| 6 | Role of Tissue Factor in Cancer | 2.21 | 0.0227 | FGB,FGA,FGG |
| 7 | GP6 Signaling Pathway | 2.18 | 0.0222 | FGB,FGA,FGG |
| 8 | Cell Cycle: G2/M DNA Damage Checkpoint Regulation | 2.07 | 0.0408 | TOP2A,ATR |
| 9 | Netrin Signaling | 1.84 | 0.0308 | DCC,CACNA1A |
| 10 | Synaptic Long Term Depression | 1.81 | 0.0161 | IGF1R,CACNA1A,PLA2G2C |
| 11 | Glucocorticoid Receptor Signaling | 1.78 | 0.0115 | KRT9,KRT2,KRT10,FGG |
| 12 | Cardiac Hypertrophy Signaling | 1.51 | 0.0124 | IGF1R,CACNA1A,ADRA1A |
| 13 | LXR/RXR Activation | 1.34 | 0.0165 | FGA,A1BG |
| 14 | FXR/RXR Activation | 1.31 | 0.0159 | FGA,A1BG |
| 15 | GADD45 Signaling | 1.28 | 0.0526 | ATR |

P-value: Fisher's exact test; molecules: the uploaded proteins mapped to the pathway.

Table 1B

The top 15 differentially deregulated pathways and related proteins in BCP 80-200 versus BCP 200-500 blood composites after TMT labeling and albumin depletion

© 2000-2019 QIAGEN. All rights reserved.

| | Ingenuity Canonical Pathways | -log(p-value) | Ratio | Molecules |
|----|--|----------------------|--------------|---|
| 1 | Acute Phase Response Signaling | 20.1 | 0.0966 | FN1,C3,C1S,APOA2,AMBP,FGG,C5,C4A/C4B,PLG,C1R,KLKB1,HP,ALB,APOA1,ITIH2,ITIH4,FGB |
| 2 | Complement System | 18.9 | 0.297 | C4A/C4B,C1R,C3,C1S,C8B,C1QC,C1QA,C1QB,C8A,C8G,C5 |
| 3 | LXR/RXR Activation | 14.4 | 0.0992 | C4A/C4B,KNG1,HPR,ALB,C3,APOA1,ITIH4,APOA2,AMBP,APOC1,CLU,APOC3 |
| 4 | FXR/RXR Activation | 14.2 | 0.0952 | C4A/C4B,KNG1,HPR,ALB,C3,APOA1,ITIH4,APOA2,AMBP,APOC1,CLU,APOC3 |
| 5 | Coagulation System | 10.8 | 0.2 | KNG1,PLG,F12,KLKB1,SERPINC1,FGB,FGG |
| 6 | Intrinsic Prothrombin Activation Pathway | 8.36 | 0.143 | KNG1,F12,KLKB1,SERPINC1,FGB,FGG |
| 7 | Extrinsic Prothrombin Activation Pathway | 6.76 | 0.25 | F12,SERPINC1,FGB,FGG |
| 8 | IL-12 Signaling and Production in Macrophages | 6.3 | 0.0473 | ALB,APOA1,APOA2,APOC1,MST1,CLU,APOC3 |
| 9 | Atherosclerosis Signaling | 5.44 | 0.0469 | ALB,APOA1,APOA2,APOC1,CLU,APOC3 |
| 10 | Production of Nitric Oxide and Reactive Oxygen Species in Macrophages | 4.39 | 0.0306 | ALB,APOA1,APOA2,APOC1,CLU,APOC3 |
| 11 | Clathrin-mediated Endocytosis Signaling | 4.24 | 0.0287 | ALB,APOA1,APOA2,APOC1,CLU,APOC3 |
| 12 | Role of Pattern Recognition Receptors in Recognition of Bacteria and Viruses | 4.06 | 0.036 | C3,C1QC,C1QA,C1QB,C5 |
| 13 | Glucocorticoid Receptor Signaling | 3.05 | 0.0173 | ERCC3,KRT9,PRKAA2,TAT,KRT2,FGG |
| 14 | Actin Cytoskeleton Signaling | 3.05 | 0.0216 | ROCK1,KNG1,FN1,GSN,TTN |
| 15 | Systemic Lupus Erythematosus Signaling | 3 | 0.0212 | KNG1,C8B,C8A,C8G,C5 |

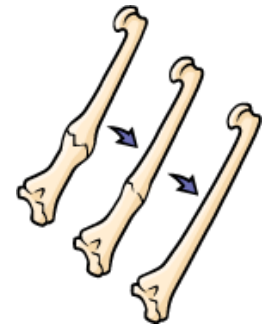
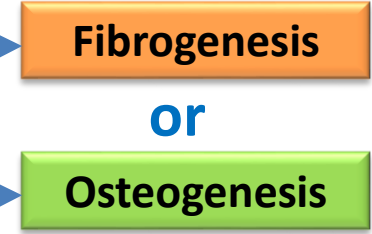
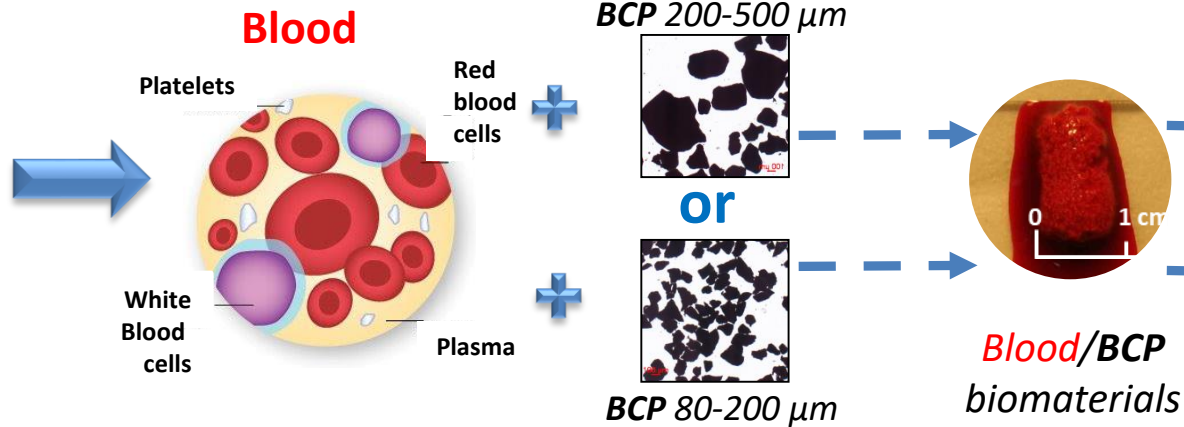
P-value: Fisher's exact test; molecules: the uploaded proteins mapped to the pathway.

Critical size bone fracture

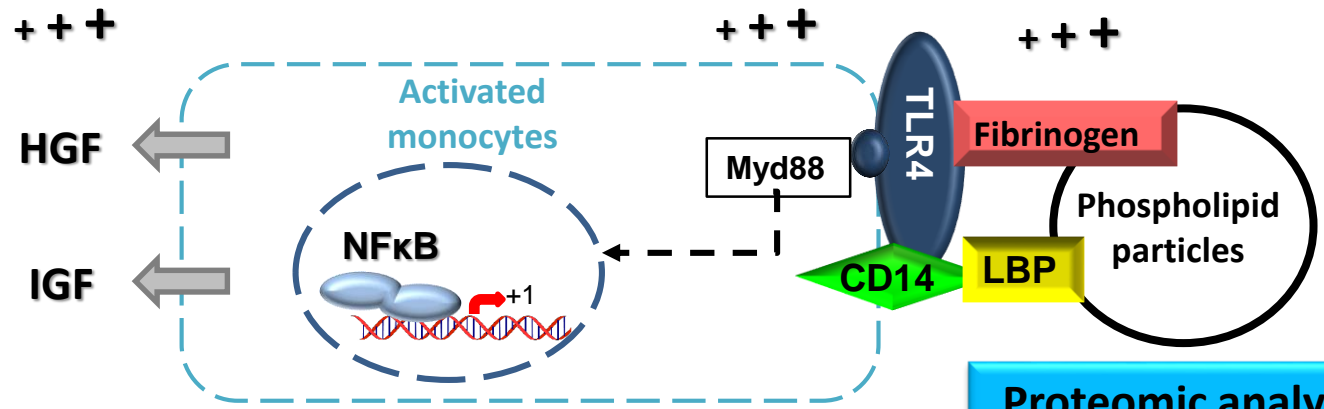


Bone Tissue Engineering

Blood/Biomaterial interactions



Bone healing



Proteomic analyses

